# The Chemistry of a 1,5-Diblocked Flavin. 2. Proton and Electron Transfer Steps in the Reaction of Dihydroflavins with Oxygen

**Gert Eberlein and Thomas C. Bruice***

*Contribution from the Department of Chemistry, University of California at Santa Barbara, Santa Barbara, California 93106.* *Received February 7, 1983*

**Abstract:** Thin-layer cyclic voltammetry has been employed to determine the pH dependence of the stepwise one-electron reduction potentials of a number of isoalloxazines [1,10-ethanolumiflavin (**1**), 1,10-ethano-5-ethyllumiflavin (**2**), 3-methyllumiflavin, 3-(carboxymethyl)lumiflavin, tetraacetylriboflavin, $N^5$-ethyl-3-methyllumiflavin (**3**), 10-(2,6-dimethylphenyl)-5-ethyl-3-methylisoalloxazine (**4**), and 1-carba-1-deaza-5-ethyl-3-methyllumiflavin (**5**)]. The Nernst plots for 3-methyllumiflavin, 3-(carboxymethyl)lumiflavin, and tetraacetylriboflavin were found to be comparable to that of FMN previously determined by Draper and Ingram. From the one-electron reduction potentials for both oxidized flavin → flavin radical and flavin radical → 1,5-reduced flavin plus the one-electron reduction potential for $O_2 \rightarrow O_2^{-}\cdot$ and $O_2^{-}\cdot \rightarrow H_2O_2$ there were calculated the standard free energies for the reactions 1,5-reduced flavin + $O_2$ → flavin radical + $O_2^{-}\cdot$ ($\Delta G^\circ_1$) and flavin radical + $O_2^{-}\cdot$ → flavin + $H_2O_2$ ($\Delta G^\circ_2$). Plots of $\Delta G^\circ_1$ vs. pH were found to parallel in shape plots of $\Delta G^{\ddagger}_f$ vs. pH for the bimolecular $O_2$ oxidation of 1,5-reduced 5-ethyl-3-methyllumiflavin. From these plots it can be seen that the free energy content of the transition state ($\Delta G^{\ddagger}_f$) exceeds the free energy content of the $O_2^{-}\cdot$ + flavin radical pairs ($\Delta G^\circ_1$) by 15 kJ $M^{-1}$. The values of $\Delta G^{\ddagger}_f - \Delta G^\circ_1$ equal the free energies of activation for reduction of flavin radicals by $O_2^{-}\cdot$ ($\Delta G^{\ddagger}_r$). Since $\Delta G^{\ddagger}_f \gg \Delta G^{\ddagger}_r$, the critical transition state for the reaction of $O_2$ with 1,5-dihydro-5-ethyl-3-methyllumiflavin must closely resemble a {flavin radical $O_2^{-}\cdot$} pair (pH range 3–10.5). The pH dependence of the apparent second-order rate constant for reaction of 1,5-dihydro-5-ethyl-3-methyllumiflavin with $O_2$ is quantitatively explained by the assumption of second-order reactions of neutral ($k_a$) and anionic ($k_b$) dihydroflavin species with $O_2$. The numerical values of $k_a$ and $k_b$ are such that the fraction $HO_2\cdot/O_2^{-}\cdot$ produced as intermediates are as predicted from the $pK_a$ of $HO_2\cdot$. The mechanism of the reaction of the 1,5-reduced **1–5** with $O_2$ was studied at pH 4.6 ($pK_a$ of $HO_2\cdot$). As in the instance of $N^5$-ethyl-3-methyllumiflavin, values of $\Delta G^\circ_1$ and $\Delta G^\circ_2$ were calculated from one-electron reduction potentials of oxygen and flavin species, $\Delta G^{\ddagger}_f$ by kinetic studies, and $\Delta G^{\ddagger}_r$ as the difference $\Delta G^{\ddagger}_f - \Delta G^\circ_1$. In all instances $\Delta G^{\ddagger}_f \gg \Delta G^\circ_2$ so that flavin radical/superoxide pairs serve as reasonable intermediates. The study with 1,5-reduced **2** ($\mathbf{2}_{red}$) was particularly rewarding since the reaction of $\mathbf{2}_{red}$ + $O_2$ is nonautocatalytic, being first order in both components. Also, $\mathbf{2}_{red}$ does not possess covalently bound protons that can be transferred to $O_2^{-}\cdot$ within the radical pair {$\mathbf{2}_{rad}$ $O_2^{-}\cdot$}. The reaction of $\mathbf{2}_{red}$ with $O_2$ is neither general- nor specific-acid catalyzed (as is true of all the 1,5-dihydroflavin oxidations of this study). The rate constant for {$\mathbf{2}_{rad}$ $O_2^{-}\cdot$} → $\mathbf{2}_{red}$ + $O_2$ (from $\Delta G^{\ddagger}_r$) equals $\sim 10^{11}$ $s^{-1}$. It follows that further reaction of {$\mathbf{2}_{rad}$ $O_2^{-}\cdot$} must occur by radical coupling to yield the flavin 4a-hydroperoxide anion 4a-**2**-$OO^-$, which may then be protonated to yield 4a-**2**-OOH. For the $O_2$ oxidation of the 1,5-reduced forms of **1** and **3–5**, it can also be shown that proton transfer to oxygen cannot occur prior to the coupling of flavin radical with $O_2^{-}\cdot$ to yield flavin 4a-hydroperoxide anions. The fitting of the initial rates for $O_2$ oxidation of 1,5-dihydrolumiflavin by a kinetic rate law is used to show that the second-order reaction of simple dihydroflavins with $O_2$ cannot be derived from initial rates due to the very early onset of autocatalysis. The reactions of the four classes of 1,5-dihydroisoalloxazines (normal, 1 blocked, 5 blocked, and 1,5 diblocked) with $O_2$ are discussed separately.

The mechanism of the bimolecular reaction of 1,5-dihydroflavins with $^3O_2$ (eq 1) is certainly not understood, though much effort

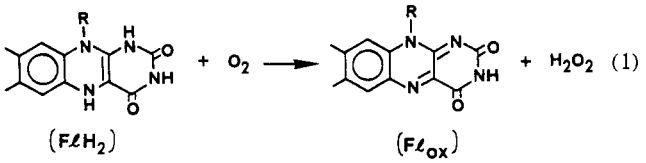


has been expended in its study.[1,2] Because it is only the initiation step in an autooxidation sequence, direct observations on the reaction of eq 1 cannot be made. Autooxidation is due, in part, to the greater rate of reaction of $Fl_{ox}$ with $FlH_2$ and $FlH^-$ as compared to the reaction of $FlH_2$ or $FlH^-$ with $^3O_2$.[1] In addition, the rate constants for the reaction of neutral and anionic flavin radicals ($FlH\cdot$ and $Fl^{-}\cdot$) with $^3O_2$ are greater than the rate constants for reaction of $FlH_2$ and $FlH^-$ with $^3O_2$. The second-order rate constant for the reaction of $Fl^{-}\cdot$ with $^3O_2$ has been reported[3] to be $\sim 10^8$ $M^{-1}$ $s^{-1}$. The autoxidation of 1,5-dihydroflavins by $O_2$ involves reactions of the type shown in eq 4.[1c] The reaction

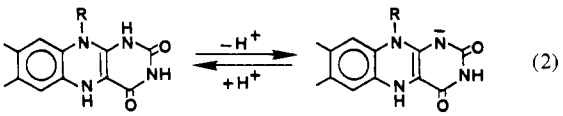


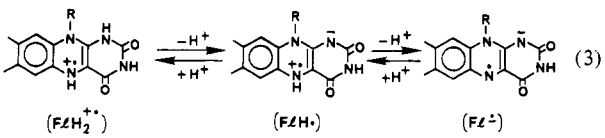


$$FlH_2 + O_2 \rightarrow Fl_{ox} + H_2O_2 \quad (4a)$$

$$FlH_2 + Fl_{ox} \rightarrow 2FlH\cdot \quad (4b)$$

$$FlH\cdot + O_2 \rightarrow Fl_{ox} + O_2^{-}\cdot + H^+ \quad (4c)$$

$$FlH\cdot + O_2^{-}\cdot \xrightarrow{H^+} Fl_{ox} + H_2O_2 \quad (4d)$$

steps of eq 4 have been substantiated by kinetic studies that include the establishment of the catalytic effect of $Fl_{ox}$ and $O_2^{-}\cdot$. In any event, the reaction of interest (eq 1 and 4a) accounts for only the first few percent of $Fl_{ox}$ appearance. For this reason, the exploration of the isolated bimolecular reaction of $O_2$ with $FlH_2$ (or $FlH^-$) is difficult.

Detailed investigations of the oxidation of $N^5$-alkyl-1,5-dihydroflavins (FlRH and $FlR^-$) by $O_2$ have been carried out in this laboratory and found to be autocatalytic in aqueous solvent.[4] In

(1) (a) Gibson, G. H.; Hastings, J. W. *Biochem. J.* **1962**, *83*, 368. (b) Massey, V.; Palmer, G.; Ballou, D. "Flavins and Flavoproteins"; Kamin, H., Ed.; University Park Press: Baltimore, MD, 1971; p 349. (c) Massey, V.; Palmer, G.; Ballou, D. "Oxidases and Related Redox Systems"; King, J. E.; Mason, H. S.; Morrison, M., Eds.; University Park Press: Baltimore, MD, 1973; Vol. I, p 25.

(2) Favaudon, V. *Eur. J. Biochem.* **1977**, *78*, 293.

(3) Faraggi, M.; Hemmerich, P.; Pecht, I. *FEBS Lett.* **1975**, *51*, 47.

0002-7863/83/1505-6685$01.50/0 

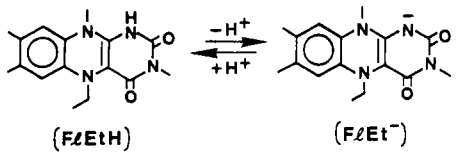


(FlEtH) (FlEt⁻) (5)

solvents of lower dielectric constant ($CH_3OH$, *t*-BuOH, dimethylformamide) there could be identified as a product the 4a-hydroperoxyflavin of eq 6.[5] At high initial concentrations of

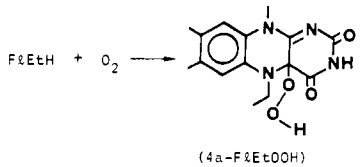


(6)

$O_2$ the 4a-FlEtOOH is observed as the most prominent oxidation product (MeOH solvent), while at low $[O_2]$ the 4a-FlEtOOH species in consumed due to its rapid reaction with reduced flavin (eq 7b).[4] The observation of the formation of 4a-FlEtOOH does

$$\text{FlEtH} + O_2 \rightarrow \text{4a-FlEtOOH} \quad (7a)$$

$$\text{FlEtH} + \text{4a-FlEtOOH} \rightarrow \text{Fl}_{ox}{}^{+}\text{Et} + \text{4a-FlEtOH} + HO^- \quad (7b)$$

$$\text{Fl}_{ox}{}^{+}\text{Et} + \text{FlEtH} \rightarrow 2\text{FlEt}\cdot + H^+ \quad (7c)$$

$$\text{FlEt}\cdot + \text{4a-FlEtOOH} \rightarrow \text{Fl}_{ox}{}^{+}\text{Et} + \text{4a-FlEtOH} + HO\cdot \quad (7d)$$

not completely clarify the mechanism of reaction of $O_2$ with 5-alkyl-1,5-dihydroflavins. Thus, the reduction of $O_2$ by FlEtH may be represented as a two-electron reduction of $O_2$ by FlEtH, yielding $H_2O_2$ and oxidized flavin ($Fl_{ox}{}^{+}Et$), followed by nucleophilic addition of $H_2O_2$ to $Fl_{ox}{}^{+}Et$ (eq 8). The synthesis of

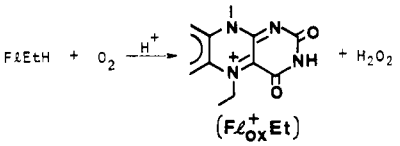


(8a)

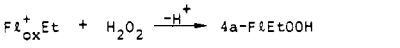


(8b)

4a-FlEtOOH is routinely carried out in this laboratory by addition of $Fl_{ox}{}^{+}Et$ to a cooled buffered solution of $H_2O_2$.[6] Arguments for two-electron reduction of $O_2$ by 1,5-dihydroflavins have been presented in the literature.[7,8] Alternatively, one may envision a two-electron reduction of $O_2$ with the direct formation of the 4a-hydroperoxide or an alternative covalent intermediate (as a 4a,10a-dioxetane)[7] that rearranges to a 4a-hydroperoxyflavin. The formation of 4a-hydroperoxyflavin might also occur following a one-electron transfer from 1,5-dihydroflavin to $O_2$ to yield flavin radical and $O_2^{-}\cdot$, which then couple. Though $O_2^{-}\cdot$ rarely behaves as a radical in coupling reactions, it has been shown that $O_2^{-}\cdot$ couples with $N^5$-ethylflavin radical (eq 9)[9] and paraquat radical[10] to yield hydroperoxides.

$$\text{FlEt}\cdot + O_2^{-}\cdot \rightarrow \text{4a-FlEtOO}^- \quad (9)$$

The objective of the present investigation has been to clarify certain mechanistic details of the reaction of 1,5-dihydroflavins with $O_2$ in aqueous solution. Of particular concern has been the role of flavin radical and $O_2^{-}\cdot$ as intermediates and the question of whether 4a-hydroperoxyflavin or $HO_2^-$ is an intermediate. For this purpose the 1,10-ethano-5-ethyllumiflavins ($\mathbf{2}_{ox}$, $\mathbf{2}_{red}$, and $\mathbf{2}_{rad}$)[11]

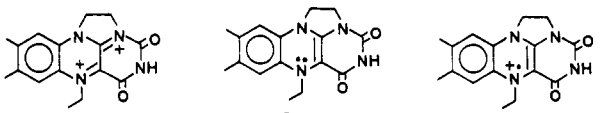

$\mathbf{2}_{ox}$ $\mathbf{2}_{red}$ $\mathbf{2}_{rad}$

have been of particular utility since by their use the oxidation reaction may be studied in $H_2O$ without the interference of an autocatalytic reaction. Thus, it has been possible to study the direct bimolecular reaction (eq 1 and 4a) of $O_2$ with the $N^5$,$N^1$-diblocked 1,5-dihydroflavin $\mathbf{2}_{red}$. By doing so certain conclusions have been reached concerning both electron and proton transfer steps. Investigations have been extended to $O_2$ oxidation of $N^1$- and $N^5$-blocked dihydroflavins and to simple 1,5-dihydroflavins. Our approach to the problem has been to employ both electrochemistry and kinetics. From these studies it is abundantly clear that the rate-determining step in the oxidation of 1,5-dihydroisoalloxazines involves electron transfer that is not preceded or accompanied by proton transfer and that an isoalloxazine hydroperoxide is a requisite intermediate.

## Experimental Section

**Materials. 1,10-Ethanolumiflavin (1), 1,10-ethano-5-ethyllumiflavin ($\mathbf{2}_{ox}$), 1,10-ethano-5-ethyllumiflavinylium cation perchlorate ($\mathbf{2}_{rad}$), and 1,5-dihydro-1,10-ethano-5-ethyllumiflavin ($\mathbf{2}_{red}$)** were obtained by the methods described in the preceding paper.[11] Unless stated otherwise, other ring-substituted isoalloxazines employed herein were from previous studies.[4,5c,12]

**10-(2,6-Dimethylphenyl)-5-ethyl-3-methyl-1,5-dihydroisoalloxazine (4)** was synthesized from 10-(2,6-dimethylphenyl)-3-methylisoalloxazine by a method similar to the procedure for **2**. 10-(2,6-Dimethylphenyl)-3-methylisoalloxazine[12] (328 mg, 0.99 mmol) was dissolved in 230 mL of 100% ethanol by ultrasonic agitation for 20 min, and 300 mg of 10% Pd/C plus 0.7 mL of 70% perchloric acid was added. The mixture was stirred magnetically in a round-bottom flask fitted with a rubber septum. After 30 min of bubbling $H_2$ through the solution using Teflon needle inlet and outlets, all flavin was reduced and no yellow or green color remained. After addition of 6 mL of 99% acetaldehyde ($1.1 \times 10^{-1}$ mol) the Teflon needle outlet was connected to a Hg gauge and the $H_2$ pressure brought to 150 torr. After 2 h another 6 mL of acetaldehyde was added. The formation of **4** was followed by withdrawing 0.1-mL aliquotes of the reaction solution, diluting with 3 mL of air-saturated ethanol, and determining the concentration of the flavin radical formed by one-electron oxidation of **4** ($\lambda_{max}$ = 463 nm, $\epsilon = \sim 8000$). After 18 h the reductive alkylation was completed. The reaction flask was transferred to an inert atmosphere glovebox (oxygen concentration $< 7 \times 10^{-8}$ M). The catalyst was removed by filtration and the excess solvent removed at elevated temperature and reduced pressure until precipitation occurred. The white precipitate was collected by filtration and washed 5 times with 30 mL of oxygen-free water until the crystals turned yellow and the effluent became neutral. The collected Pd/C catalyst was washed with chloroform until the effluent became colorless. The aqueous filtrate and wash were combined and adjusted to pH 4.5 with sodium carbonate and acetate buffer. The slightly acidic solution was extracted with the Pd/C/chloroform wash solution. The aqueous phase was discarded and the chloroform fraction dried over anhydrous sodium carbonate. After filtration and evaporation of the chloroform, the remaining residue was dissolved in ethanol. Water was then added until a bright yellow precipitation commenced (several days). In this manner 140 mg of **4** was obtained (67% yield), mp 256–285 °C.

**Electrochemistry.** The reduction potentials for the flavins reported herein were determined by use of the thin-layer cyclic voltammetry technique of Hubbard.[13] The number of electrons transferred in a reversible process was determined from the equation $n = Q/(FVC)$ (*F*

(4) For a detailed study see: Kemal, C.; Chan, T. W.; Bruice, T. C. *J. Am. Chem. Soc.* **1977**, *99*, 7272.
(5) (a) Reference 4 and prior references contained herein. (b) Iwata, M.; Bruice, T. C.; Carrell, H. L.; Glusker, J. P. *J. Am. Chem. Soc.* **1980**, *102*, 5036. (c) Ball, S.; Bruice, T. C. *J. Am. Chem. Soc.* **1981**, *103*, 5494.
(6) Kemal, C.; Bruice, T. C. *Proc. Natl. Acad. Sci. U.S.A.* **1976**, *73*, 995.
(7) Orf, H. W.; Dolphin, D. *Proc. Natl. Acad. Sci. U.S.A.* **1974**, *71*, 2646.
(8) Hemmerich, P.; Bhaduri, A. P.; Blankenhorn, G.; Brustlein, M.; Haas, W.; Knappe, W.-R. "Oxidases and Related Redox Systems"; King, T. E.; Morrison, M.; Mason, H. S., Eds.; University Park Press: Baltimore, MD, 1973; Vol. I, Chapter I.
(9) Nanni, J. E.; Sawyer, D. T.; Ball, S. S.; Bruice, T. C. *J. Am. Chem. Soc.* **1981**, *103*, 2797.
(10) Nanni, J. E.; Angelis, C. T.; Dickson, J.; Sawyer, D. T. *J. Am. Chem. Soc.* **1981**, *103*, 4268.
(11) Eberlein, G.; Bruice, T. C. *J. Am. Chem. Soc.*, **1983**, preceding paper in this issue. A portion of this material has appeared in preliminary form: *J. Am. Chem. Soc.* **1982**, *104*, 1449.
(12) Main, L.; Kasperek, G. J.; Bruice, T. C. *Biochemistry* **1972**, *11*, 3991.
(13) Hubbard, A. T. *CRC Crit. Rev. Anal. Chem.* 1973, *3* (2), 201–242. Hubbard, A. T. *J. Electroanal. Chem. Interfacial Electrochem.* **1969**, *22*, 165.

= Faraday, $9.66 \times 10^4$ A $s^{-1}$ $M^{-1}$; $V$ = volume of capillary cell, $4.66 \times 10^{-6}$ L; $C$ = concentration of species, M) where $Q$ is the charge transferred per sweep which is equal to $AXY/\nu$ [A = integrated area under the peak, $X$ = units of the $x$ axis (V $cm^{-1}$), $Y$ = units of the $y$ axis (A $cm^{-1}$), and $\nu$ = scan speed (V $s^{-1}$)]. The determination of the integrated area under the reduction peak was carried out by digitizing the CV curve and calculating the area by using a Hewlett-Packard calculator. The redox potentials were determined at four or more different values of pH and the $E^0$ potentials employed were obtained from the best computer fit of the Nernst equation to the experimental $E_m$ values. Operations were carried out under $N_2$ with $N_2$-purged solutions at 23–24 °C with a scan rate of 1 mV $s^{-1}$ unless otherwise specified. Scanning was to negative field employing a 0.75-V scan range at a sensitivity of 0.01 mA. The working electrode employed was iodide coated before each measurement. The reference employed was AgCl/1 M NaCl (reference potential 0.225 V vs. NHE at 25 °C). All potentials are given vs. NHE. To maintain pH the following buffers were employed: $H_0 = -0.22$, 1 M perchloric acid; pH 1.3, 1/9 0.25 M sulfate buffer and 1 M sodium perchlorate; pH 4.6, 1/9 2 M acetate buffer and 1 M sodium perchlorate; pH 6.7, 1/9 0.25 M phosphate buffer and 1 M sodium perchlorate. $Me_2SO$ or $CH_3CN$ was added up to 50% as required by the solubility of the isoalloxazine. In separate experiments it was found that the addition of these solvents did not influence values of $E_m$.

**Kinetics.** In **the reaction of 2 with oxygen**, the desired volumes of $O_2$-saturated and $N_2$-saturated buffers (pH 4.6) were placed into a cuvette by injection through a rubber septum cap. After thermal equilibration in the cell compartment of the spectrophotometer, there was added 0.1 mL of an anaerobic methanolic solution 2.7 mM in $\mathbf{2}_{red}$ (final solution $8.7 \times 10^{-5}$ M in **2**, 3.2% (v/v) acetonitrile/methanol). The solution was mixed and the appearance of $\mathbf{2}_{rad}$ followed with time at 492 nm. The reaction of $\mathbf{4}_{red}$ with $O_2$ was carried out in a similar manner and the formation of the oxidation product followed at 484 nm (appearance of the radical).

To determine the initial rate constant of the reaction of $O_2$ with the flavins $\mathbf{1}_{red}$, $\mathbf{3}_{red}$, and $\mathbf{5}_{red}$ equal volumes of oxygen-saturated acetate buffer ($\mu$ = 1.0) and 1,5-dihydroflavin ($\sim 5 \times 10^{-5}$ M) were mixed together on the stopped-flow bench. The reactions were followed at 585 nm (5-ethyl-3-methyllumiflavin), 444 nm (3-methyllumiflavin), and 365 nm (1-deaza-1-carba-6-ethyl-3-methyllumiflavin). The tangential slopes for the first 3–5% of reaction were employed to calculate the initial rate constants.

**Hydrogen peroxide** product was determined by withdrawing 0.4 mL of the reaction solution and adding this to 3 mL of aqueous and oxygen-free 0.1 M sodium iodide solution. The appearance of $I_3^-$ was monitored with time at 358 nm ($\epsilon$ = 25 000 $M^{-1}$ $cm^{-1}$). The time course for $I_3^-$ appearance was found to be biphasic. The rapid first-order production of $I_3^-$ due to the presence of $H_2O_2$ is followed by a much slower production of $I_3^-$ due to the $O_2$ present in the reaction solution as a reagent. The time course for $I_3^-$ formation due to $H_2O_2$ was isolated by use of a computer program for consecutive (pseudo-) first-order reactions. Thus, the $[I_3^-]$ formed from reaction with $H_2O_2$ could be calculated as could the second-order rate constant for the reaction of $I^-$ with $H_2O_2$. The rate constants so determined were found to be identical with the second-order rate constant for reaction of $I^-$ with authentic $H_2O_2$ at the pH employed ($k_2$ = 156 $M^{-1}$ $s^{-1}$).

**Apparatus.** Electrochemical measurements were carried out with a modified Princeton Applied Research Model 174 polarographic analyzer with a modified cyclic voltammetry circuit and thin-layer platinum cyclic voltammetry electrodes designed by Professor A. T. Hubbard. Kinetic studies were carried out by use of Thunberg techniques and a Cary-118C spectrophotometer or by use of a Durram (D-110) stopped-flow spectrophotometer with ~2-ms dead time and 4.6-ms mixing time. The stopped-flow spectrophotometer was sealed in a glovebox under nitrogen ($[O_2] \sim 5 \times 10^{-8}$ M). Spectrophotometric p$K_a$ values were determined as described previously.[11]

## Results

**Electrochemical redox potentials of representative members of four types of isoalloxazines** have been determined. The four classes of isoalloxazines considered are (i) unblocked with tetraacetylriboflavin, 3-(carboxymethyl)lumiflavin and 3-methyllumiflavin as examples, (ii) $N^5$-blocked with $N^5$-ethyl-3-methyllumiflavin as the example, (iii) $N^1$-blocked with 1,10-ethanolumiflavin as the example, and (iv) $N^1$,$N^5$-diblocked with 1,10-ethano-5-ethyllumiflavin as the example. The electrochemical redox potentials for these isoalloxazines have been determined as a function of pH by employing thin-layer cyclic voltammetry with a platinum billet electrode (vs. NHE, 23 ± 1 °C).

In Figure 1 there is shown the pH dependence of thin-layer cyclic voltammograms (TLCV) for 3-methyllumiflavin and tetraacetylriboflavin. Inspection of Figure 1 reveals that the TLCVs exhibit single transfer waves for oxidation and reduction between pH 12.4 and pH 1.1. From the areas under the anodic and cathodic peaks it is determined that each peak potential is associated with the transfer of two electrons. Further, the anodic and cathodic peak potentials are separated on the average by 74 mV (pH 1.1–12.4) so that the reductions are essentially thermodynamically and electrochemically reversible. Below pH 1.1 the TLCV for 3-methyllumiflavin exhibits two anodic and two cathodic peak potentials that are separated by 9 mV and are each associated with one-electron transfer. In Figure 2A is presented a Nernst plot derived from the pH dependence of the one-electron and two-electron transfer potentials of 3-methyllumiflavin, 3-(carboxymethyl)lumiflavin, and tetraacetylriboflavin (the latter only to pH 8). The derived Nernst plot is essentially identical with the experimentally determined plots for one-electron and

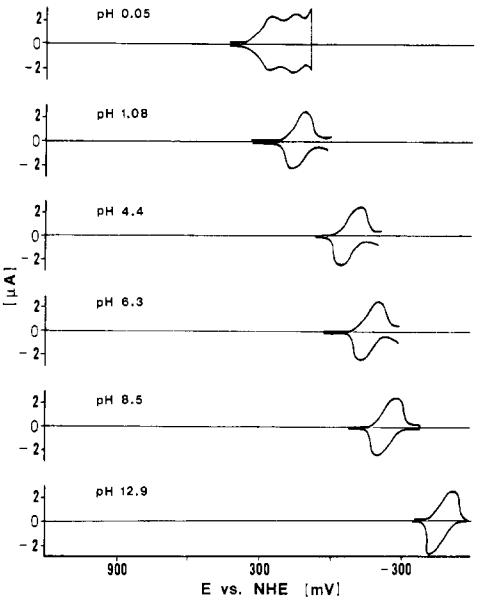


**Figure 1.** pH dependence of the thin-layer cyclic voltammograms for 3-methyllumiflavin (pH 0.05, $\mu$ = 2.0) and tetraacetylriboflavin (remaining pH values, $\mu$ = 1.0) determined at a scan speed of 1 mV/s (solvent $H_2O$; 23 °C with flavin at $\sim 9 \times 10^{-4}$ M). Direction of scan is from positive to negative potential. The areas under the curves associated with the peak potentials for anodic and cathodic scans integrate on the average to 2.1 electrons. The partial separation to two one-electron transfer steps is seen at pH 0.05.

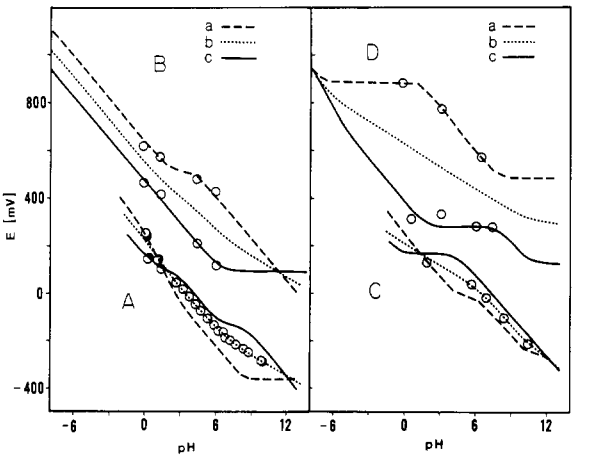


**Figure 2.** Nernst-Clark plots of potential vs. pH. Lines a, b, and c represent one-electron reduction of oxidized flavin, two-electron reduction of oxidized flavin, and one-electron reduction of flavin radical, respectively. Plot A is for 3-methyllumiflavin, 3-(carboxymethyl)lumiflavin, and tetraacetylriboflavin (only to pH 8 for this flavin). Plot B is for 5-ethyl-3-methyllumiflavin. Plot C is for 1,10-ethanolumiflavin and plot D is for 1,10-ethano-5-ethyllumiflavin.

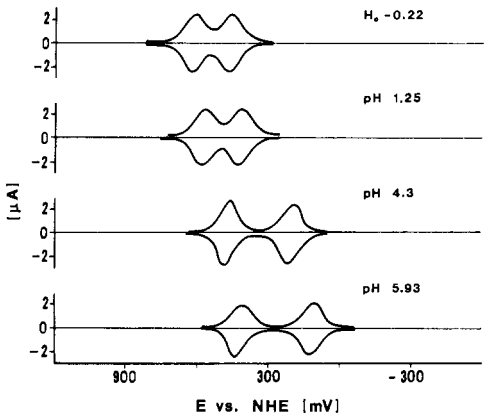


**Figure 3.** pH dependence of thin-layer cyclic voltammograms for $N^5$-ethyl-3-methyllumiflavin ($\sim 5.5 \times 10^{-4}$ M) at a scan speed of 1 mV/s (solvent $H_2O$; $\mu$ = 1.0; 23 °C). Direction of scan is from positive to negative. For pH 5.93 and 4.3 the areas under the curves associated with the two peak potentials for anodic and the two peak potentials for cathodic sweeps integrate on the average to 0.88 ± 0.17 each. The total areas for anodic and cathodic sweeps at pH 1.25 and $H_0$ = −0.22 integrate on the average to 2.12 ± 0.16. In these instances there are seen two anodic and two cathodic peak potentials, which shows that one-electron transfer is associated with each peak.

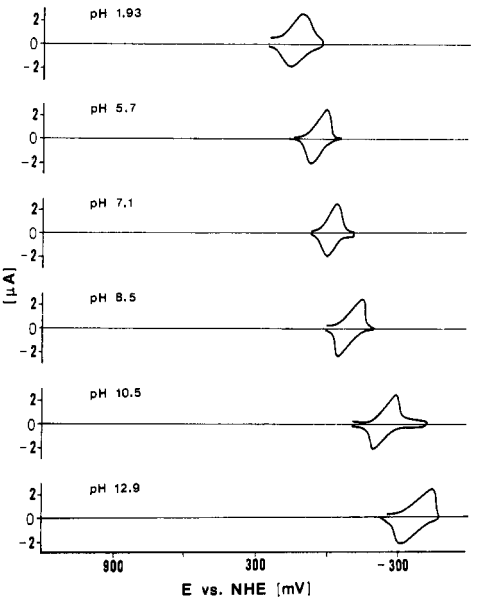


**Figure 4.** pH dependence of the thin-layer cyclic voltammograms for 1,10-ethanolumiflavin ($1.9 \times 10^{-4}$ M) at a scan speed of 1 mV/s (solvent at pH 1.93 is 44% $Me_2SO/H_2O$ (v/v) and at pH 5.1–12.9 it is 44% $CH_3CN/H_2O$ (v/v); $\mu$ = 0.5; 23 °C). Direction of scan is from positive to negative. The area under the anodic and cathodic sweeps integrates on the average to 2.09 ± 0.44.

## Scheme I

(I) For one-electron reduction of oxidized flavin

$$E_m = E_0 + \frac{RT}{F} \ln \left( \frac{[H^+]^2 + [H^+]K_1 + K_1K_2}{[H^+] + K_3} \right) - \frac{RT}{F} \ln \left( \frac{1 + K_1 + K_1K_2}{1 + K_3} \right)$$

(II) For one-electron reduction of flavin radical

$$E_m = E_0 + \frac{RT}{F} \ln \left( \frac{[H^+]^3 + [H^+]^2K_4 + [H^+]K_4K_5 + K_4K_5K_6}{[H^+]^2 + [H^+]^1K_1 + K_1K_2} \right) - \frac{RT}{F} \ln \left( \frac{1 + K_4 + K_4K_5 + K_4K_5K_6}{1 + K_1 + K_1K_2} \right)$$

(III) For two-electron reduction of oxidized flavin

$$E_m = E_0 + \frac{RT}{2F} \ln \left( \frac{[H^+]^3 + [H^+]^2K_4 + [H^+]K_4K_5 + K_4K_5K_6}{[H^+]^2 + [H^+]K_7 + K_7K_3} \right) - \frac{RT}{2F} \ln \left( \frac{1 + K_4 + K_4K_5 + K_4K_5K_6}{1 + K_7 + K_7K_3} \right)$$

where

(a) $FlH_2^{+\cdot} \overset{K_1}{\rightleftharpoons} H^+ + FlH\cdot$ $pK_1$ = 2.3 (ref 17)

(b) $FlH\cdot \overset{K_2}{\rightleftharpoons} H^+ + Fl^{-\cdot}$ $pK_2$ = 8.27 (ref 15)

(c) $Fl_{ox}H^+ \overset{K_3}{\rightleftharpoons} H^+ + Fl_{ox}$ $pK_3$ = 0.18 (ref 16)

(d) $FlH_3^+ \overset{K_4}{\rightleftharpoons} H^+ + FlH_2$ $pK_4$= 0.8 (ref 18)

(e) $FlH_2 \overset{K_5}{\rightleftharpoons} H^+ + FlH^-$ $pK_5$ =6.25 (ref 15)

(f) $FlH^- \overset{K_6}{\rightleftharpoons} H^+ + Fl^{2-}$ $pK_6 > 16$ (ref 19)

(g) $Fl_{ox}H_2^{2+} \overset{K_7}{\rightleftharpoons} H^+ + Fl_{ox}H^+$ $pK_7 = -7.79$ (ref 11)

two-electron transfer to riboflavin and FMN (to pH 8) made by Draper and Ingraham.[14] The equations and constants employed to generate the plot of Figure 2A are shown in Scheme I. The equations of Scheme I (and Schemes II–IV) are of a general form provided by Clark[15] but appended to be useful for acid dissociation constants in the $H_0$ range.

In Figure 3 there is shown the acidity constant dependence of the TLCV for $N^5$-ethyl-3-methyllumiflavin (**3**). Inspection of Figure 3 shows the presence of two anodic and two cathodic waves at each acidity. Integration of the area under each peak potential curve establishes that reduction and oxidation are associated with two separate one-electron transfers. The separation of the anodic and cathodic peaks, for each of the two one-electron transfer processes, establishes their kinetic and thermodynamic reversibility. Thus, viewed in the direction of the cathodic sweep, the separation of the cathodic and anodic peak potentials are as follows: pH −0.22, 6 and 6 mV; pH 1.25, 24 and 11 mV; pH 4.3, 33 and 27 mV; pH 5.93, 30 and 21 mV (all scan speeds 1 mV/s). No attempts at studies of TLCV at high pH values were made due to possible complexities due to addition of $HO^-$ to the 4a-position of the oxidized species (Scheme II, reaction b). A Nernst plot of midpoint potentials vs. acidity functions for $N^5$-ethyl-3-methyllumiflavin is presented in Figure 2B. Equations employed in the generation of the lines of Figure 2B are provided in Scheme II. The $pK_a$ for pseudobase formation (Scheme II, eq b) is seen to be reflected in the Nernst plot for the one-electron reduction

(14) Draper, R. D.; Ingraham, L. L. *Arch. Biochem. Biophys.* **1968**, *125*, 802–808.
(15) Clark, W. M. "Oxidation Reduction Potentials of Organic Systems"; R. E. Creiger: Huntington, NY, 1972; p 129.
(16) Schollnhammer, G.; Hemmerich, P. *Eur. J. Biochem.* **1974**, *44*, 561–577.
(17) Land, E. J.; Swallow, A. J. *Biochemistry* **1969**, *8*, 2117–2125.
(18) Hemmerich, P.; Ghisla, S.; Hartmann, U.; Muller, F. "Flavins and Flavoproteins"; Kamin, H., Ed.; University Park Press: Baltimore, MD, 1971; pp 83–103.
(19) Exact value does not influence calculation.
(20) Schug, C. Diplomarbeit, University of Konstanz, West Germany, 1978; p 34.
(21) Ghisla, S.; Hartmann, U.; Hemmerich, P.; Muller, F. *Justus Liebigs Ann. Chem.* **1973**, 1388–1415.
(22) Kemal, C.; Bruice, T. C. *J. Am. Chem. Soc.* **1976**, *98*, 3955.
(23) Porter, D. J. T.; Voet, J. G.; Bright, H. J. *J. Biol. Chem.* **1973**, *248*, 4400–4416.
(24) Determined by spectrophotometric titration: G. Eberlein and T. C. Bruice, unpublished experiments.
(25) Usual value for $N^1$-protonation of a reduced flavin.

**Scheme II**

(I) For one-electron reduction of oxidized 5-ethyl-3-methyllumiflavin

$$E_m = E_0 + \frac{RT}{F}\ln\left(\frac{[H^+]^2 + [H^+]K_1 + K_1K_2}{[H^+] + K_3}\right) - \frac{RT}{F}\ln\left(\frac{1 + K_1 + K_1K_2}{1 + K_3}\right)$$

(II) For one-electron reduction of semireduced 5-ethyl-3-methylflavinylium radical

$$E_m = E_0 + \frac{RT}{F}\ln\left(\frac{[H^+]^3 + [H^+]^2K_4 + [H^+]K_4K_5 + K_4K_5K_6}{[H^+]^2 + [H^+]K_1 + K_1K_2}\right) - \frac{RT}{F}\ln\left(\frac{1 + K_4 + K_4K_5 + K_4K_5K_6}{1 + K_1 + K_1K_2}\right)$$

(III) For two-electron reduction of oxidized 5-ethyl-3-methyllumiflavin

$$E_m = E_0 + \frac{RT}{2F}\ln\left(\frac{[H^+]^2 + [H^+]K_4 + K_4K_5}{[H^+] + K_3}\right) - \frac{RT}{2F}\ln\left(\frac{1 + K_4 + K_4K_5}{1 + K_3}\right)$$

where

a) 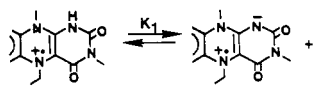 $pK_1$ = 2.06 (ref. 20)

b) 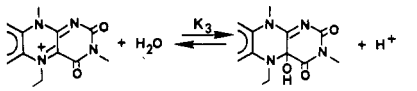 $pK_3$ = 4.0 (ref 21,22)

c) 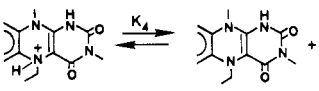 $pK_4$ = 1.94 (ref 20)

d) 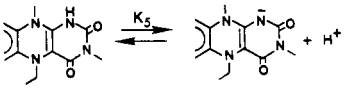 $pK_5$ = 6.4 (ref 23)

$pK_2$ for radical and $pK_6$ for reduced >16 (ref 19)

**Scheme III**

(I) For one-electron reduction of oxidized 1,10-ethanolumiflavin

$$E_m = E_0 + \frac{RT}{F}\ln\left(\frac{[H^+]^4 + [H^+]^3K_1 + [H^+]^2K_1K_2 + [H^+]K_1K_2K_3 + K_1K_2K_3K_4}{[H^+]^3 + [H^+]^2K_5 + [H^+]K_5K_6 + K_5K_6K_7}\right) - \frac{RT}{F}\ln\left(\frac{1 + K_1 + K_1K_2 + K_1K_2K_3 + K_1K_2K_3K_4}{1 + K_5 + K_5K_6 + K_5K_6K_7}\right)$$

(II) For one-electron reduction of 1,10-ethanolumiflavinylium radical

$$E_m = E_0 + \frac{RT}{F}\ln\left(\frac{[H^+]^3 + [H^+]^2K_8 + [H^+]K_8K_9 + K_8K_9K_{10}}{[H^+]^2 + [H^+]K_2 + K_2K_3}\right) - \frac{RT}{F}\ln\left(\frac{1 + K_8 + K_8K_9 + K_8K_9K_{10}}{1 + K_2 + K_2K_3}\right)$$

(III) For two-electron reduction of oxidized 1,10-ethanolumiflavin

$$E_m = E_0 + \frac{RT}{2F}\ln\left(\frac{[H^+]^4 + [H^+]^3K_8 + [H^+]^2K_8K_9 + [H^+]K_8K_9K_{10} + K_8K_9K_{10}K_{11}}{[H^+]^3 + [H^+]^2K_5 + [H^+]K_5K_6 + K_5K_6K_7}\right) - \frac{RT}{2F}\ln\left(\frac{1 + K_8 + K_8K_9 + K_8K_9K_{10} + K_8K_9K_{10}K_{11}}{1 + K_5 + K_5K_6 + K_5K_6K_7}\right)$$

where

(a) 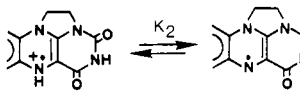 $pK_2$ = 4.4 (ref 20)

(b) 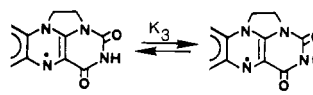 $pK_3$ = 10.2 (ref 20)

(c) 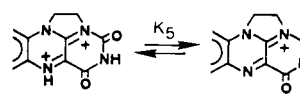 $pK_5$ = -8.43 (ref 11)

(d) 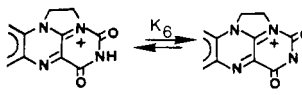 $pK_6$ = 6.1 (ref 20)

(e) 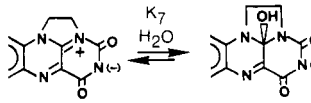 $pK_7$ = 12.18 (ref 24)

(f) 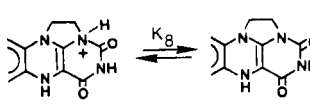 $pK_8$ = -0.50 (ref 25)

(g) 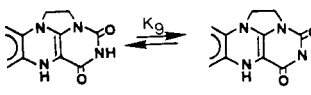 $pK_9$ = 9.9 (ref 20)

$pK_{10}$ and $pK_{11}$ reduced form >16 (ref 19)

$pK_1$ of radical form $\leq -1.50$

**Scheme IV**

(I) For one-electron reduction of oxidized 1,10-ethano-5-ethyllumiflavin dikathion ($\mathbf{2}_{ox}^{2+}$)

$$E_m = E_0 + \frac{RT}{F}\ln\left(\frac{[H^+]^2 + [H^+]K_1 + K_1K_2}{[H^+]K_4}\right) - \frac{RT}{F}\ln\left(\frac{1 + K_1 + K_1K_2}{K_4}\right)$$

(II) For one-electron reduction of 1,10-ethano-5-ethyllumiflavinylium radical

$$E_m = E_0 + \frac{RT}{F}\ln\left(\frac{[H^+]^3 + [H^+]^2K_5 + [H^+]K_5K_6 + K_5K_6K_7}{[H^+]^2 + [H^+]K_1 + K_1K_2}\right) - \frac{RT}{F}\ln\left(\frac{1 + K_5 + K_5K_6 + K_5K_6K_7}{1 + K_1 + K_1K_2}\right)$$

(III) For two-electron reduction of oxidized 1,10-ethano-5-ethyllumiflavinium dicathion ($\mathbf{2}_{ox}^{2+}$)

$$E_m = E_0 + \frac{RT}{2F}\ln\left\{\frac{[H^+]^3 + [H^+]^2K_5 + [H^+]K_5K_6 + K_5K_6K_7}{[H^+]^2 + [H^+]K_3 + K_3K_4}\right\} - \frac{RT}{2F}\ln\left\{\frac{1 + K_5 + K_5K_6 + K_5K_6K_7}{1 + K_3 + K_3K_4}\right\}$$

where

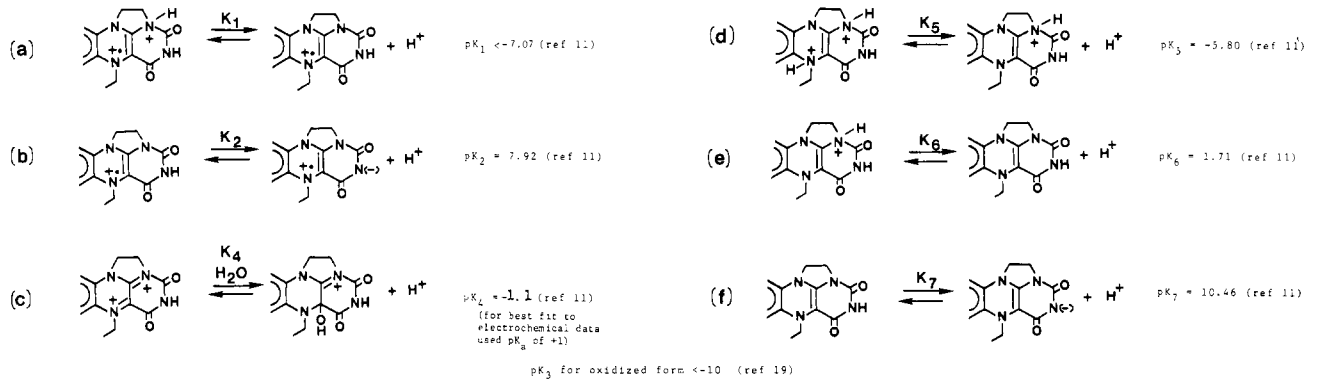


of **3**. That the pseudobase formation does not interfere with the kinetic reversibility (at moderate pH) of the reduction of **3** at the Pt electrode indicates that the equilibrium for reaction b (Scheme II) is maintained during the anodic reduction using a sweep time of 1 mV/s.

The pH dependence of the TLCV for 1,10-ethanolumiflavin (**1**) is shown in Figure 4. It is seen that anodic and cathodic sweeps are both associated with one peak potential at all pH values employed. Integration of the areas under both anodic and cathodic nodes show that two electrons are transferred. The separation of the peak potentials in sweeping in the cathodic direction (1 mV/s) are constant with an increase in pH until high pH (pH 1.93, 51 ΔmV; pH 5.70, 48 ΔmV; pH 7.10, 39 ΔmV; pH 8.50, 54 ΔmV; pH 10.50, 45 ΔmV; pH 12.90, 78 ΔmV). The finding of the small differences of the peak potentials (ΔmV) at all pH values indicates a thermodynamically and electrochemically reversible system. The increased separation of anodic and cathodic sweep maximum at pH 12.9 may be related to the formation of a 10a-pseudobase (eq e, Scheme III). In Figure 2C there is shown the Nernst plot for the redox reactions of the 1,10-ethanolumiflavin system (Scheme III).

Thin-layer cylic voltammograms for 1,10-ethano-5-ethyllumiflavin (**2**) are shown in Figure 5. Attention is drawn to the TLCV at pH 3.1, which was obtained at a scan speed of 2 mV/s in a cathodic sweep. The first peak potential relates to the reduction of the chemically unstable dication $\mathbf{2}_{ox}$. Extrapolation and integration of the area under the peak potential in the anodic direction for this wave indicate the transfer of ~0.64 electron. All this is in accord with the instability of $\mathbf{2}_{ox}$ in the pH range and the very low $pK_a$ for its pseudobase formation ($pK_a = -1.1$).[11] The second set of peak potentials obtained at pH 3.1 pertain to the reduction of the radical. At this pH, and all pH values investigated, the integrated area indicated the transfer of one electron. The reduction of the radical species is thermodynamically and kinetically reversible at all pH values investigated (ΔmV = 35). The acidity dependence of the redox potentials for the 1,10-ethano-5-ethyllumiflavin system is shown in Figure 2D. The lines of Figure 2D have been generated as shown in Scheme IV.

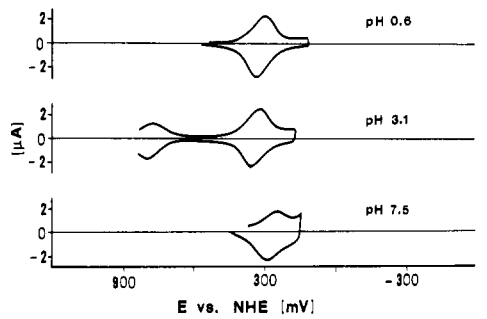


**Figure 5.** pH dependence of the thin-layer cyclic voltammograms for 1,10-ethano-5-ethyllumiflavin ($7.0 \times 10^{-4}$ M) at a scan speed of 2 mV/s (solvent $H_2O$; 23 °C). Direction of scan is from positive to negative. At pH 0.6 ($\mu = 0.5$) and pH 7.5 ($\mu = 1.0$) the scan is started from positive to negative after reduced flavin has been converted to its radical at the electrode. At these pH values the scans represent one-electron reduction of flavin radical to reduced flavin. At pH 3.3 ($\mu = 0.7$), reduced flavin was converted to the oxidized form on the electrode prior to scanning. Separate potential waves are seen for reduction of oxidized flavin to flavin radical and reduction of flavin radical to reduced flavin. The area under the curves associated with both anodic and cathodic peak potentials integrate on the average to 0.85 ± 0.12.

**The reaction of $\mathbf{2}_{red}$ with molecular oxygen was studied between pH 1.0 and pH 6.0** (30 ± 0.2 °C, $\mu = 1$ with KCl, $H_2O$ solvent) by the mixing of anaerobic solutions of $\mathbf{2}_{red}$ ($5 \times 10^{-5}$ to $1 \times 10^{-6}$ M) with solutions of known $[O_2]$. The radical $\mathbf{2}_{rad}$ was found to be the sole product detectable by visible spectroscopy. Above pH 6.0 the radical undergoes disproportionation (see preceding paper in this issue)[11] at a rate sufficient to becloud the use of $\mathbf{2}_{rad}$ formation as a means of following $\mathbf{2}_{red}$ oxidation in the neutral and basic pH range.

Under the pseudo-first-order conditions of $[O_2] \gg [\mathbf{2}_{red}]$ the formation of $\mathbf{2}_{rad}$ followed the first-order rate law in the pH range of 1–6. Furthermore, at a constant oxygen concentration of $4 \times 10^{-4}$ M the pseudo-first-order rate constants were found to be identical within experimental error over a change of $[H_3O^+]$ of

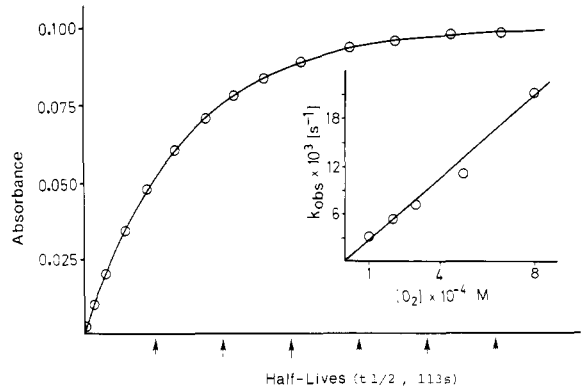


**Figure 6.** First-order appearance of 1,10-ethano-5-ethylflavinium radical (**4**) on oxidation of 1,10-ethano-5-ethyl-1,5-dihydrolumiflavin (at $1.1 \times 10^{-5}$ M, 30 °C, pH 1.8, with $[O_2] = 3 \times 10^{-4}$ M). Points are experimental and the line theoretical for a first-order rate constant ($k_{obsd}$) of $5.66 \times 10^{-3}$ s$^{-1}$. The inset is a plot of $k_{obsd}$ vs. $[O_2]$ with a slope of 25 M$^{-1}$ s$^{-1}$.

10 000-fold. Changes of buffer concentration [($CH_3COO^-$/$CH_3COOH$) and ($SO_4^{2-}$/$HSO_4^-$)] over the 20-fold range of 0.1–2 M at constant pH values and constant oxygen concentration did not influence the rate of appearance of $\mathbf{2}_{rad}$. The fact that the reaction of $\mathbf{2}_{red}$ with oxygen is pseudo first order to six to eight half-lives is remarkable in the literature of 1,5-dihydroflavin–oxygen chemistry. In Figure 6 there is shown a first-order plot obtained for the reaction of $\mathbf{2}_{red}$ ($1.1 \times 10^{-5}$ M) with $O_2$ ($3 \times 10^{-4}$ M) at pH 1.8. In the inset to Figure 6 there is plotted the pseudo-first-order rate constants ($k_{obsd}$) vs. the concentrations of oxygen employed. The slope of the plot provides the second-order rate constant of 22 M$^{-1}$ s$^{-1}$. In like experiments, the second-order rate constant for reaction of $\mathbf{2}_{red}$ with oxygen at pH 4.7 was determined as 17 M$^{-1}$ s$^{-1}$. In these experiments, the solutions of various oxygen concentrations were prepared by diluting an oxygen-saturated buffer solution with one saturated with nitrogen. The concentration of oxygen was calculated by assuming that the oxygen-saturated solution was $8 \times 10^{-4}$ M in oxygen.[26] When employing ordinary laboratory-grade methanol as the solvent, the reaction of $\mathbf{2}_{red}$ with oxygen is slow ($t_{1/2} \sim 60$ min). In the purified organic solvents MeOH, $CH_3CN$, and *t*-BuOH, $\mathbf{2}_{red}$ is not oxidizable by $^3O_2$ at an observable rate.

For the reaction of $\mathbf{2}_{red}$ with oxygen in water, analysis for hydrogen peroxide product was carried out by an iodometric procedure (see Experimental Section). The percentage yield of hydrogen peroxide based of [$\mathbf{2}_{red}$] employed was 50% (45%, 52%, 47%, 47%, 47%). That the product responsible for $I^-$ oxidation was indeed hydrogen peroxide was established by the finding that the pseudo-first-order rate constant for $I_3^-$ formation with a sample of reaction solution was identical with that observed when an authentic solution of hydrogen peroxide was employed.

**The rate constants for the reaction of oxygen with 5-ethyl-3-methyl-1,5-dihydrolumiflavin** were obtained from tangents drawn to the initial absorbance vs. time plots for the appearance of the flavin radical. These experiments were carried out by rapid mixing on the stopped-flow bench of oxygen-saturated acetate buffer ($\mu$ = 1.0 with KCl) with nitrogen-saturated acetate buffer containing the dihydroflavin. Apparent second-order rate constants were calculated from tangential initial rates and $[O_2]$. The second-order rate constant at pH 4.6 was found to be 49 M$^{-1}$ s$^{-1}$. The time course for reaction of 1,5-dihydro-3,5-dimethyllumiflavin ($FlHCH_3$) with oxygen as a function of pH was previously investigated by Kemal, Chan, and Bruice (Scheme V).[4] The rates of oxidation of $FlHCH_3$, as in the instance of other dihydroflavins,[1] were found to be sensitive to pH due to acid/base equilibria of the dihydroflavin moiety. However, neither specific-acid nor general-acid catalysis was found to be involved.[4,5c] The initial rate constants determined in this study with $\mathbf{3}_{red}$ were also found to be insensitive to buffer catalysis between pH 1 and pH 5. The

(26) Chan, R. L.; Bruice, T. C. *J. Am. Chem. Soc.* **1978**, *100*, 7.

Scheme V

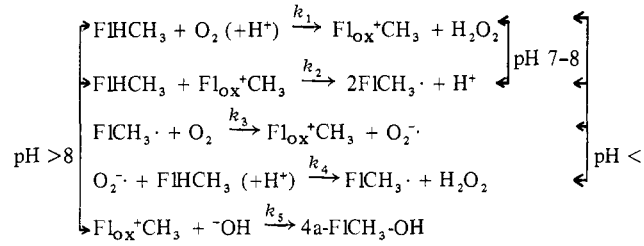


calculated second-order rate constants for reaction of $O_2$ with $FlHCH_3$ and $\mathbf{3}_{red}$ as determined from initial rates are the same within experimental error. Thus, substitution of –Et for –Me at the N$^5$-position of 1,5-dihydro-3-methyllumiflavin does not alter the reactivity with $O_2$.

**The rate constants for the reaction of $O_2$ with a number of selected 1,5-dihydroflavins** were also obtained by stopped-flow studies at pH 4.6 and taken as tangents to plots of flavin absorbance vs. time for the first few percent oxidation. Second-order rate constants determined from initial rates and $[O_2]$ are as follows: for 1,5-dihydro-3-methyllumiflavin, 417 M$^{-1}$ s$^{-1}$; for 1,5-dihydro-1,10-ethanolumiflavin ($\mathbf{1}_{red}$), 1500 M$^{-1}$ s$^{-1}$; for 1,5-dihydro-10-(2,6-dimethylphenyl)-5-ethylisoalloxazine ($\mathbf{4}_{red}$), 4.2 M$^{-1}$ s$^{-1}$; for 1-carba-1-deaza-5-ethyl-3-methyllumiflavin ($\mathbf{5}_{red}$), 42 M$^{-1}$ s$^{-1}$.

## Discussion

Cyclic voltammetry, when employing the thin-layer technique of Hubbard,[14] may be used to determine not only the apparent thermodynamic potentials for a reversible reaction but also the number of electrons transferred in a particular redox step. In this study we have applied this technique (TLCV) in the determination of the pH dependence of the one- and two-electron reduction potentials of a number of flavins. The potentials determined with 3-(carboxymethyl)lumiflavin, tetraacetyllumiflavin, riboflavin, and FMN fit the same Nernst plot as does 3-methyllumiflavin (between pH 7 and $H_0 = -0.22$). Electrochemical reduction of these flavins as well as 1,10-ethanolumiflavin ($\mathbf{1}_{ox}$) and oxidation of their 1,5-dihydroflavin forms occur by a two-electron process due to the instability of the intermediate radical species (eq 10). The

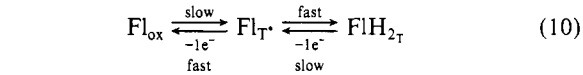

(10)

stabilizing influence of an N$^5$-substituent upon the flavin radical[4] is illustrated by the TLCV of 5-ethyl-3-methyllumiflavin ($\mathbf{3}_{ox}$) and 5-ethyl-1,10-ethanolumiflavin ($\mathbf{2}_{ox}$), which are reduced in two one-electron steps. The potentials associated with $\mathbf{2}_{ox} \rightarrow \mathbf{2}_{rad}$ (eq 11) are more positive than any redox potential previously measured

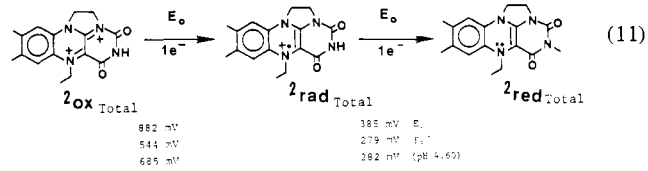

(11)

for an isoalloxazine molecule (either free in solution or enzyme bound). From the Nernst plot of the potentials of eq 11 vs. acidity functions (Figure 2C) it may be seen that the intercrossing of the potential vs. acidity curves for the first and second electron transfer processes is not expected until high proton activity is obtained ($H_0 = -7$). For this reason, the disproportionation of $\mathbf{2}_{rad}$ (eq 12)

$$2\mathbf{2}_{rad} \rightleftarrows \mathbf{2}_{ox} + \mathbf{2}_{red} \quad (12)$$

should not be thermodynamically favorable above an $H_0$ of about –7. In the preceding paper[11] we show that the solvolytically driven disproportionation (eq 13) is unimportant in the acid pH range.

$$2\mathbf{2}_{rad} \rightleftarrows \mathbf{2}_{ox} + \mathbf{2}_{red}$$
$$2_{ox} \xrightarrow{\text{solvolysis}} \text{products} \quad (13)$$

Scheme VI. pH 4.6; at pH = p$K_a$ of HOO·

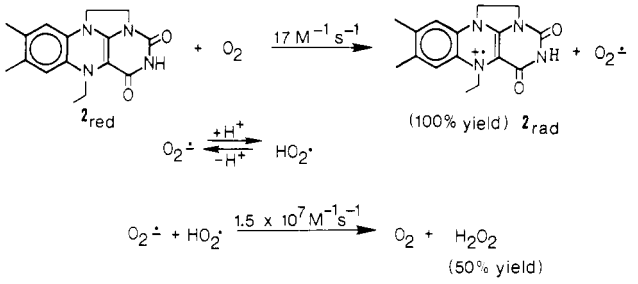


Thus, $\mathbf{2}_{rad}$ is a stable species in mildly acidic to strongly acidic solution.

Both electrochemical and **kinetic studies of the $O_2$ oxidation of 1,10-ethano-5-ethyl-1,5-dihydrolumiflavin ($\mathbf{2}_{red}$)** establish that studies with this particular dihydroflavin allow the most unambiguous conclusions concerning the mechanism of $O_2$ oxidation of the dihydroflavins. All other 1,5-dihydroflavins examined to date undergo an autocatalytic oxidation by $O_2$ (eq 4 and 7). Autocatalysis (see Results) is not seen in the reaction of $\mathbf{2}_{red}$ with $^3O_2$. In what follows the mechanism of reaction of $\mathbf{2}_{red}$ with $O_2$ will be discussed first followed by a discussion of the oxidation of 1,5-dihydro $N^5$-blocked flavins and an $N^1$-blocked flavin and in turn the mechanism of oxidation of nonblocked 1,5-dihydroflavins will be considered.

The reaction of $\mathbf{2}_{red}$ with oxygen has been found to be first order in both [$\mathbf{2}_{red}$] and [$O_2$] to provide the flavin radical $\mathbf{2}_{rad}$ in 100% yield and $H_2O_2$ in 50% yield (based upon the initial concentrations of $\mathbf{2}_{red}$ employed)—eq 14 and 15. Several mechanisms may be

$$\mathbf{2}_{red} + O_2 \xrightarrow{H^+} \mathbf{2}_{rad} + {}^1/_2H_2O_2 \qquad (14)$$

$$\frac{-d[\mathbf{2}_{red}]}{dt} = k_{ox}[2_{red}][O_2] \qquad (15)$$

considered. These appear to be kinetically equivalent but may be differentiated on the basis of the electrochemical data. The first mechanism is provided in Scheme VI (the standard conditions of pH 4.6 and 1 M in reactants and products have been chosen for these studies). According to the sequence of Scheme VI, $\mathbf{2}_{red}$ transfers an electron to $O_2$ to yield $\mathbf{2}_{rad}$ and $O_2^{-}\cdot$. This reaction would be required to be rate determining. It is known that $O_2^{-}\cdot$ reduces $N^5$-ethylflavin radical (at least in aprotic solvent).[9] To prevent reversal of the reduction of $O_2$ by $\mathbf{2}_{red}$, $O_2^{-}\cdot$ rapidly becomes protonated and converted to the products $H_2O_2$ plus $O_2$ by disproportionation. Since the reaction of $\mathbf{2}_{red}$ with $O_2$ has been studied at a pH equivalent to the p$K_a$ of HOO·, the conditions are optimum for the protonation of $O_2^{-}\cdot$ and its disproportionation. The reasonableness of Scheme VI may be evaluated by the use of electrochemical data.

The standard potentials for reduction of $^3O_2$ to $O_2^{-}\cdot$ have been determined in a number of investigations.[27] The standard potentials of eq 16 have been corrected to pH 4.6 by use of the Nernst

| | $E_0$ (pH 4.6) | |
|---|---|---|
| $O_2$ + 1e⁻ → Superoxide | −310 mV | (16a) |
| superoxide + 1e⁻ → hydrogen peroxide | 1203 mV | (16b) |

equation. By combination of $E_0$ (pH 4.6) of eq 16a with the $E_0$ (pH 4.6) for one-electron reduction of $\mathbf{2}_{rad}$ (eq 11), there is obtained eq 17

$$\mathbf{2}_{red} + O_2 \rightleftarrows \mathbf{2}_{rad} + O_2^{-}\cdot \qquad \text{emf (pH 4.6)} = -594 \text{ mV} \qquad (17)$$

from which there is obtained the equilibrium constant of eq 18.

$$\mathbf{2}_{red} + O_2 \overset{K_e}{\rightleftharpoons} \mathbf{2}_{rad} + O_2^{-}\cdot \quad K_e = 1.3 \times 10^{-10} \qquad (18)$$

(27) (a) Rabani, J.; Matheson, M. S. *J. Am. Chem. Soc.* **1964**, *86*, 3175. (b) Koppenol, W. H. *Nature (London)* **1976**, *262*, 420. (c) Koppenol, W. H. *Photochem. Photobiol.* **1978**, *28*, 431. (d) George, P. "Oxidases and Related Redox Systems"; King, T. D.; Mason, H. S.; Morrison, M., Eds.; Wiley: New York, 1965; Vol. I, p 3.

Scheme VII. pH 4.6

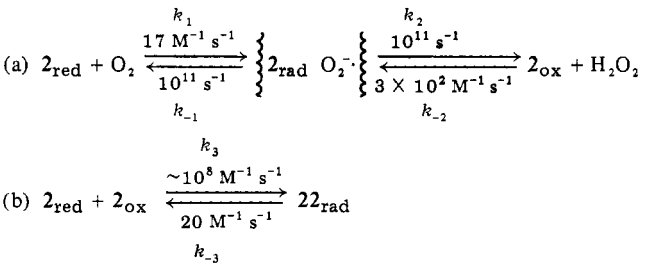


Scheme VI may be abbreviated as in eq 19 where $k_{ox}$ = 17 $M^{-1}$

$$\mathbf{2}_{red} + O_2 \overset{K_e}{\rightleftharpoons} \mathbf{2}_{rad} + O_2^{-}\cdot$$

$$2O_2^{-}\cdot \xrightarrow[\text{pH 4.6}]{k_r} H_2O_2 + O_2 \qquad (19)$$

$s^{-1} = K_e k_r$ and $k_r$ must then equal $10^{11}$ $M^{-1}$ $s^{-1}$. Obviously, the sequence of reactions composing Scheme VI is not kinetically competent since $k_r$ would be required to exceed a diffusion-controlled reaction. Also, $k_r$ would represent rate-determining protonation of $O_2^{-}\cdot$ or equilibrium protonation of $O_2^{-}\cdot$ and rate-determining reaction of $O_2^{-}\cdot$ with $HO_2\cdot$. The pseudo-first-order rate constant for protonation of $O_2^{-}\cdot$ at pH 4.6 equals but 2.5 × $10^5$ $s^{-1}$.

By combination of the standard potentials for one-electron reduction of $O_2^{-}\cdot$ at pH 4.6 (eq 16b) with the standard potential for one-electron reduction of $\mathbf{2}_{ox}$ to yield $\mathbf{2}_{rad}$, there is obtained the potential of eq 20.

$$\mathbf{2}_{rad} + O_2^{-}\cdot \overset{\text{pH 4.6}}{\rightleftharpoons} \mathbf{2}_{ox} + H_2O_2 \qquad \text{emf (pH 4.6)} = 518 \text{ mV} \qquad (20)$$

Combination of the electrochemical cells of eq 17 and eq 20 provides eq 21.

$$\mathbf{2}_{red} + O_2 \overset{\text{pH 4.6}}{\rightleftharpoons} \mathbf{2}_{ox} + H_2O_2 \text{emf (pH 4.6)} = -76 \text{ mV} \qquad (21)$$

From eq 21 it follows that the adjusted (to pH 4.6) standard free energy for the overall reaction of eq 21 is +7.3 kJ $M^{-1}$. The overall reaction of $\mathbf{2}_{red}$ with $O_2$ to provide $\mathbf{2}_{ox}$ and $H_2O_2$ is then slightly endothermic, and barring a trapping of $\mathbf{2}_{ox}$, the reaction should not be favorable. The reaction of oxidized and reduced $N^5$-alkyl flavins to provide flavin radical (an example is seen in eq 7c) is exergonic and rapid.[4,22] Unreacted reduced flavin ($\mathbf{2}_{red}$) could act as a trap of the endergonically produced $\mathbf{2}_{ox}$ of eq 21. If this were so, $\mathbf{2}_{ox}$ would only exist as an intermediate in the formation of $\mathbf{2}_{rad}$ (eq 22). The determined second-order rate constant $k_{ox}$ would,

$$\mathbf{2}_{red} + O_2 \xrightarrow{\text{r.d.s.}} H_2O_2 + \mathbf{2}_{ox} \qquad (22a)$$

$$\mathbf{2}_{red} + \mathbf{2}_{ox} \rightarrow 2\mathbf{2}_{rad} \qquad (22b)$$

according to eq 22, pertain to the two-electron reduction of $O_2$ by $\mathbf{2}_{red}$. If $\mathbf{2}_{rad}$ and $O_2^{-}\cdot$ were intermediates in the reaction of eq 22a, then Scheme VII would be in effect. In Scheme VII the constant $k_1$ equals the experimentally determined second-order rate constant $k_{ox}$ ($\Delta G^{\ddagger}$ = 67 kJ $M^{-1}$) and $k_{-1}$ has been calculated from $\Delta G^{\ddagger} - \Delta G^{\circ}$ where $\Delta G^{\circ}$ pertains to the standard (pH 4.6) free energy of eq 17 ($\Delta G^{\circ}$ = 57 kJ $M^{-1}$). As the value of $k_2$ cannot far exceed $k_{-1}$, it has been assumed to be equal to $k_{-1}$. The value of $\Delta G^{\ddagger}$ associated with $k_{-2}$ is then obtained by subtracting $\Delta G^{\circ}$ (pH 4.6) for the two-electron reduction of $O_2$ by $\mathbf{2}_{red}$ (eq 22a) from $\Delta G^{\ddagger}$ determined for the reaction. In this manner, the rate constants for reaction a of Scheme VII have been derived. The equilibrium constant for reaction b of Scheme VII is calculated to be 5 × $10^6$ from the standard potentials (pH 4.6) for one-electron reduction of $\mathbf{2}_{ox}$ by $\mathbf{2}_{red}$. The second-order rate constants for reaction of oxidized and reduced flavins may be taken as ~$10^8$ $M^{-1}$ $s^{-1}$ so that by using this value for $k_3$ and the determined equilibrium constant there is obtained the rate constants of eq b of Scheme VII. As we shall see, Scheme VII is not complete.

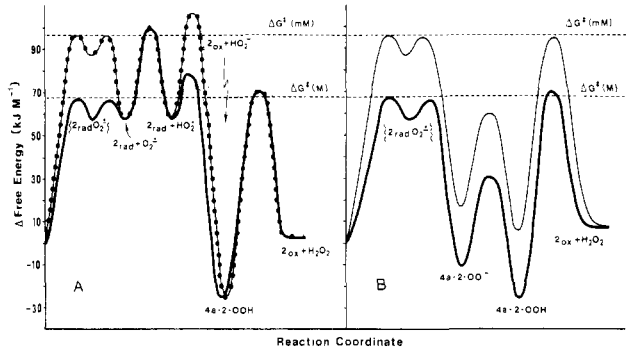


**Figure 7.** Two reaction coordinant cartoons for the oxidation of 1,5-dihydro-1,10-ethano-5-ethyllumiflavin ($\mathbf{2}_{red}$) by $O_2$ ($H_2O$; 30 °C). The plots in (A) represent the intermediate formation of the $\{\mathbf{2}_{rad}\ O_2^{-}\cdot\}$ ion pair, which dissociates to $\mathbf{2}_{rad} + O_2^{-}\cdot$ followed by diffusion-controlled protonation of $O_2^{-}\cdot$. There then follows a one-electron transfer from $\mathbf{2}_{rad}$ to $HO_2\cdot$ to provide $\mathbf{2}_{ox} + HO_2^{-}$ or the 4a-hydroperoxide of $\mathbf{2}_{ox}$ (4a-**2**-OOH) [(—) standard state 1 M; (●) standard state $10^{-3}$ M]. Rate-controlling (or partially rate controlling) steps are seen to follow the initial formation of $\{\mathbf{2}_{rad}\ O_2^{-}\cdot\}$. In plots B the radical ion pair collapses directly to form 4a-**2**-$OO^-$ in a step that does not involve proton transfer (standard state 1 M, dark line). The rate-controlling step is the formation of $\{\mathbf{2}_{rad}\ O_2^{-}\cdot\}$.

It is useful, however, to employ Scheme VII in the elaboration of the most likely mechanism.

Examination of Scheme VII shows that the rate constant for back conversion of $O_2^{-}\cdot + \mathbf{2}_{rad}$ to $O_2 + \mathbf{2}_{red}$ must exceed the rate for bimolecular diffusion. Thus, the intermediates must exist as the radical pair ($\{O_2^{-}\cdot\ \mathbf{2}_{rad}\}$) which is in free energy content 10 kJ $M^{-1}$ below the transition state for the overall rate-determining reaction. The back conversion rate of $10^{11}$ $s^{-1}$ approaches the limit of diffusion from a solvent cage.[28] The values of $E_0$ (pH 4.6) employed in the electrochemical calculation are not likely to be in error by more than 30 mV, and the rate-determining constant is known with less than 2 kJ $M^{-1}$ error. Thus, the species $\{O_2^{-}\cdot\ \mathbf{2}_{rad}\}$ is in free energy content ~10 kJ $M^{-1}$ less than that of the transition state for the rate-determining step, and the transition state must, therefore, be very similar in structure to $\{O_2^{-}\cdot\ \mathbf{2}_{rad}\}$.

The compound $\mathbf{2}_{red}$ does not possess protons that can be transferred to $O_2$ on reduction of the latter. This feature provides a unique entrance to the question of the formation of an intermediate covalent hydroperoxide in the course of reaction of $\mathbf{2}_{red} + O_2$. The oxidation of $\mathbf{2}_{red}$ by $O_2$ is not subject to either specific- or general-acid catalysis. Since $\mathbf{2}_{red}$ has no transferable protons and acid catalysis is not involved, there are no protons trapped with the $\{O_2^{-}\cdot\ \mathbf{2}_{rad}\}$ species that may be passed to $O_2^{-}\cdot$ on its reduction. Because $O_2^{2-}$ formation is associated with a very high $\Delta G°$, reduction of $O_2^{-}\cdot$ by $\mathbf{2}_{rad}$ is not possible within the solvent caged $\{O_2^{-}\cdot\ \mathbf{2}_{rad}\}$ pair. Enforced catalysis by proton transfer from a water molecule may be dismissed as a possibility. Thus, a proton transfer from $H_2O$ ($pK_a$ 15.5) to $O_2^{-}\cdot$ ($pK_a$ of HOO· is 4.7)[29] is endothermic and could not occur in an intracomplex reaction ($\{O_2^{-}\cdot\ \mathbf{2}_{rad}H_2O\}$) with a minimal rate constant of $10^{11}$ $s^{-1}$. One must conclude that neither $k_{-1}$ nor $k_2$ of Scheme VII involves a proton transfer to an oxygen species. A shortcoming of Scheme VII now becomes apparent. It does not explain the means by which the radical pair $\{\mathbf{2}_{rad}\ O_2^{-}\cdot\}$ is converted to $\mathbf{2}_{ox} + H_2O_2$.

The reaction steps of Scheme VIII may be considered for the converion of $\{\mathbf{2}_{red}\ O_2^{-}\cdot\}$ to $\mathbf{2}_{ox} + H_2O_2$. In Figure 7A there are drawn reaction coordinant cartoons for standard states of 1 and $10^{-3}$ M reactants and products at pH 4.6. Under the standard state conditions of 1 M in reactants and products employed for standard free energies, energies of activation and standard potential—i.e., reaction coordinant diagrams—there is little free energy difference between organic cation anion pairs and solvent

Scheme VIII

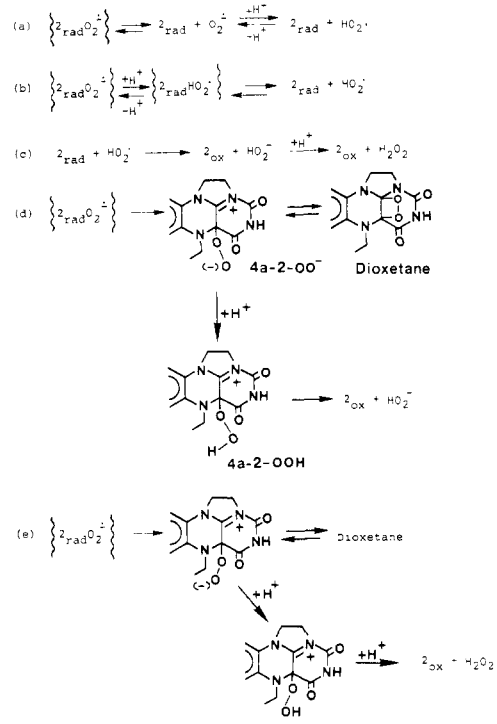


separated species.[30] For this reason the free energies of formation of $\mathbf{2}_{rad} + O_2^{-}\cdot$ at 1 M may be taken as equal to that of the paired species $\{\mathbf{2}_{rad}\ O_2^{-}\cdot\}$ and since our standard state has been chosen at pH 4.6 ≅ $pK_a$ of $H_2O\cdot$ the equilibrium constants of eq a are close to unity. However, the pseudo-first-order rate constant for the diffusion-controlled protonation of $O_2^{-}\cdot$ or $\{\mathbf{2}_{rad}\ O_2^{-}\cdot\}$ at pH 4.6 would be $2.5 \times 10^5$ $s^{-1}$. Thus, the free energy of activation for protonation of $O_2^{-}\cdot$ or $\{\mathbf{2}_{rad}\ O_2^{-}\cdot\}$ is ~43 kJ $M^{-1}$ so that protonation of these species would result in a $\Delta G^{\ddagger}$ observed equal to the standard free energy of formation of $\mathbf{2}_{rad} + O_2^{-}\cdot$ plus the kinetic free energy of protonation (57 + 43 = 100 kJ $M^{-1}$). The determined value of $\Delta G^{\ddagger}_{obsd}$ is ~67 kJ $M^{-1}$. Examination of Figure 7A shows that the transition states for $O_2^{-}\cdot$ protonation and coupling of $HO_2\cdot + \mathbf{2}_{rad}$ both exceed in free energy $\Delta G^{\ddagger}$ regardless of the standard-state concentration chosen. The formation of $\mathbf{2}_{rad} + HO_2\cdot$ must not occur and reactions a–c of Scheme VIII must be discarded. This leaves for consideration the pathways of reactions d and e. The species $HO_2^{-}$ ($pK_a$ of $H_2O_2$ is 11.6)[31] is thermodynamically unstable at pH 4.6. The $\Delta G°$ (pH 4.6) for conversion of $\mathbf{2}_{red} + O_2 \rightarrow \mathbf{2}_{ox} + HO_2^{-}$ exceeds that (7.5 kJ $M^{-1}$) for the formation of $\mathbf{2}_{ox} + H_2O_2$ by 41 kJ $M^{-1}$ so that $\Delta G°$ (pH 4.6) for the formation of $\mathbf{2}_{ox} + HO_2^{-}$ is equal to ~48.5 kJ $M^{-1}$. The free energy content of $\mathbf{2}_{ox} + HO_2^{-}$ is but 19 kJ $M^{-1}$ less than the free energy content of the transition state. The transition state for diffusion-controlled protonation of $\mathbf{2}_{ox} + HO_2^{-}$ by $H_3O^{+}$ (at pH 4.6) to yield $\mathbf{2}_{ox} + H_2O_2$ would then possess a free energy content 24 kJ $M^{-1}$ above the experimentally determined $\Delta G^{\ddagger}$ for the overall reaction and, therefore, $\mathbf{2}_{ox} + HO_2^{-}$ cannot arise along the reaction path. (These calculations pertain to a standard state of 1 M but by inspection of Figure 7A it can be seen that like conclusions are reached when 1 mM standard state is employed.) This leaves only path e of Scheme VIII as a possibility. The formation of $\mathbf{2}_{ox}$ by $O_2$ oxidation of $\mathbf{2}_{red}$ is most reasonably represented by eq 23.

$$\mathbf{2}_{red} + O_2 \rightarrow \{\mathbf{2}_{rad}\ O_2^{-}\cdot\} \rightarrow \text{4a-2-OO}^- \underset{-H^+}{\overset{+H^+}{\rightleftharpoons}} \text{4a-2-OOH} \xrightarrow{+H^+} \mathbf{2}_{ox} + H_2O_2 \quad (23)$$

(28) For a discussion of the topic, see: Murdoch, J. *J. Am. Chem. Soc.* **1980**, *102*, 71. In solvents other than water tabulated limits for diffusion apart range from $\sim 10^5$ to $10^{12}$ $s^{-1}$.

(29) Sawyer, D. T.; Valentine, J. S. *Acc. Chem. Res.* **1981**, *14*, 393–400.

(30) Harred, H. S.; Owen, B. B. "The Physical Chemistry of Electrolytic Solutions", Reinhold: New York, 1958; Chapter 7. Robinson, R. A.; Stokes, R. H. "Electrolyte Solutions"; Butterworths: London, 1959; Chapter 14.

(31) Everett, A. J.; Minkoff, G. J. *Trans. Faraday Soc.* **1953**, *49*, 410.

An approximation of the reaction coordinate diagram for the sequence of eq 23 may be constructed and is presented in Figure 7B. The standard free energies for the conversion of $\mathbf{2}_{red} + O_2 \rightarrow \{\mathbf{2}_{rad}\ O_2^{-}\cdot\}$ and $\mathbf{2}_{red} + O_2 \rightarrow \mathbf{2}_{ox} + H_2O_2$ (pH 4.6) have been calculated from the electrochemical data as before (eq 11, 17, 20, and 21). The equilibrium constant for pseudobase formation with $\mathbf{2}_{ox}$ was determined in the preceeding paper[11] as −1.1 (Scheme IV, reaction c). If it is assumed that the same equilibrium constant may be employed for reaction of $H_2O_2$ with $\mathbf{2}_{ox}$ to yield 4a-**2**-OOH, then at pH 4.6 the ratio of $[\text{4a-2-OOH}]/([\mathbf{2}_{ox}][H_2O_2]) = 5 \times 10^5$ and $\Delta G°$ for the formation of 4a-**2**-OOH from $\mathbf{2}_{red} + O_2$ is −26 kJ $M^{-1}$. An estimate of the $pK_a$ of eq 24 has been made.[32]

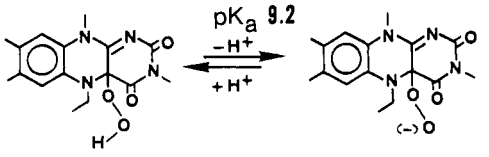


(24)

A reasonable value for the $pK_a$ of the hydroperoxy function of 4a-**2**-OOH is ~7, so that $\Delta G°$ (pH 4.6) for 4a-**2**-$OO^-$ formation from $\mathbf{2}_{red} + O_2$ is −12 kJ $M^{-1}$. A reasonable rate constant for addition of $H_2O_2$ to $\mathbf{2}_{ox} \rightarrow$ 4a-**2**-OOH + $H^+$ (pH 4.6) would[33] be 100 $M^{-1}$ $s^{-1}$ ($\Delta G^{\ddagger}$ = 63 kJ $M^{-1}$) and protonation of 4a-**2**-$OO^-$ to yield 4a-**2**-OOH would be diffusion controlled ($\Delta G^{\ddagger}$ = 43 kJ $M^{-1}$ at pH 4.6). These considerations pertain to the standard state of 1 M and provide one of the cartoons of Figure 7B. The second cartoon of Figure 7B pertains to a standard state of 1 mM. Conclusions drawn from either are basically the same. Since 4a-**2**-OOH is of greater thermodynamic stability than is $\mathbf{2}_{ox} + H_2O_2$, the formation of $\mathbf{2}_{rad}$ can take place by reaction of $\mathbf{2}_{red}$ with 4a-**2**-OOH without formation of $\mathbf{2}_{ox}$ (eq 25). The formation of

$$\mathbf{2}_{red} + O_2 \left\{ \rightleftharpoons \mathbf{2}_{rad}\ O_2^{-} \right\} \longrightarrow \text{4a-2-}OO^- \overset{+H^+}{\underset{-H^+}{\rightleftharpoons}} \text{4a-2-OOH} \quad (25)$$

$$\mathbf{2}_{red} + \text{4a-2-OOH} \xrightarrow{H^+} \mathbf{2}_{rad} + H_2O_2$$

flavin radical on reaction of a 4a-hydroperoxide with reduced flavin is a known reaction (eq 7a,b). The oxidation of $\mathbf{2}_{red}$ most likely follows the sequence of eq 25.

Within experimental error, the second-order rate constant for reaction of $\mathbf{2}_{red}$ with $O_2$ is pH insensitive. The potential for one-electron reduction of $O_2$ is, of course, pH sensitive due to the $pK_a$ values of superoxide (1.0 and 4.7).[29,34] For this reason calculated values of $\Delta G°$ for $\mathbf{2}_{rad}$ and superoxide formation by one-electron transfer from $\mathbf{2}_{red}$ to $O_2$ decrease with pH. At pH 1.8 the value of $\Delta G^{\ddagger}$ for reaction of $O_2$ with $\mathbf{2}_{red}$ exceeds $\Delta G°$ by 22 kJ $M^{-1}$. The increase in $\Delta G^{\ddagger} - \Delta G°$ on a decrease in pH below the $pK_a$ of $HO_2\cdot$ reflects the lack of a proton in the transition state for formation of $\{\mathbf{2}_{rad}\ O_2^{-}\cdot\}$ and that the calculated values of $\Delta G°$ at low pH do not represent the proper free energies of formation of the radical pair $\{\mathbf{2}_{rad}\ O_2^{-}\cdot\}$.

**The mechanism of reaction of $O_2$ with 1,5-dihydro-5-ethyl-3-methyllumiflavin ($\mathbf{3}_{red}$)** serves as an example of the reaction of an $N^5$-blocked dihydroflavin with $O_2$.[4] From the half-cell reactions of eq 16 and 26 there can be calculated the standard (pH 4.6)

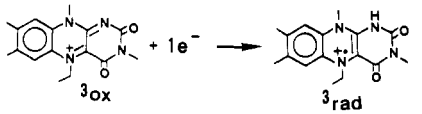


(26a)

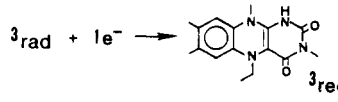


(26b)

(32) (a) Bruice, T. C. *J. Chem. Soc., Chem. Commun.*, **1983**, 14. (b) Bruice, T. C.; Noar, J. B.; Ball, S. S.; Venkataram, U. V. *J. Am. Chem. Soc.* **1983**, *105*, 2452–2463.

(33) See tabulation of pseudobase $pK_a$ values by Bunting, J. W. *Adv. Hetercycl. Chem.* **1979**, *25*, 2–79; Bunting, J. W. *Heterocycles* **1980**, *14*, 2015–2045.

(34) Rabani, J.; Nielsen, S. O. *J. Phys. Chem.* **1969**, *73*, 3736–3744. Chevalet, J.; Rouelle, F.; Gierst, L.; Lambert, J. P. *J. Electroanal. Chem. Interfacial Electrochem.* **1972**, *39*, 201–216.

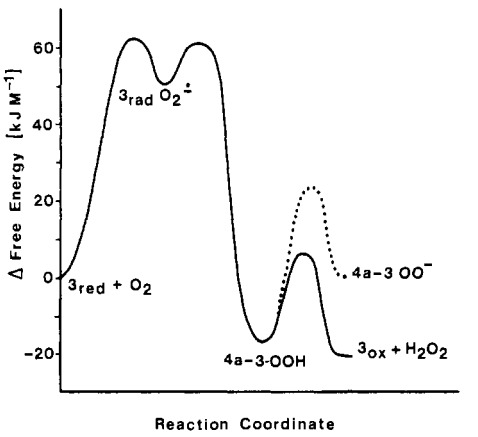


**Figure 8.** Reaction coordinate cartoon for the oxidation of $N^5$-ethyl-1,5-dihydrolumiflavin ($\mathbf{3}_{red}$) by $O_2$ at 30 °C in $H_2O$ at pH 4.6.

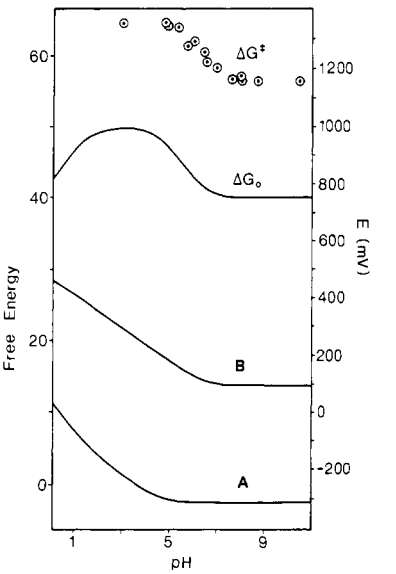


**Figure 9.** Plots of the experimentally determined free energies of activation ($\Delta G^{\ddagger}$) and calculated standard free energies ($\Delta G°$), for formation of flavin radical plus superoxide on reaction of 1,5-dihydro-5-ethyl-3-methyllumiflavin ($\mathbf{3}_{red}$) with $O_2$ (30 °C; $H_2O$) vs. pH. Lines a and b represent the pH dependencies of the $E_m$ for $O_2 + 1e^- \rightarrow O_2^{-}\cdot$ and $\mathbf{3}_{rad} + 1e^- \rightarrow \mathbf{3}_{red}$, respectively.

free energy of formation of $\mathbf{3}_{rad} + O_2^{-}\cdot$. This value is equal to 49 kJ $M^{-1}$. From initial rate measurements (see Results) the standard free energy of activation for the reaction of $\mathbf{3}_{red}$ with $O_2$ is calculated as 64 kJ $M^{-1}$ at pH 4.6. It follows that the free energy content of the transition state is but 15 kJ $M^{-1}$ greater than that of $\mathbf{3}_{rad} + O_2^{-}\cdot$ at pH 4.6. Employing the electrochemical cells of eq 26 and 16, one can calculate the standard free energy of formation of $\mathbf{3}_{ox} + H_2O_2$ from $\mathbf{3}_{red} + O_2$ as −21 kJ $M^{-1}$ at pH 4.6. Dependent upon the standard-state molarity, the free energy contents of the transition states for diffusion-controlled protonation of either $O_2^{-}\cdot$ or $HO_2^-$ or the one-electron transfer from $\mathbf{3}_{rad}$ to $HO_2\cdot$ possess free energy contents greater than that of the critical transition state for the overall reaction. Thus, $\mathbf{3}_{ox} + HO_2^-$ would not be expected to exist intermediate along the reaction coordinant. In Figure 8 there is presented a reaction coordinate cartoon for the $O_2$ oxidation of $\mathbf{3}_{red}$ at pH 4.6. The cartoon follows the sequence of eq 27. In the construction of the cartoon the pseudobase $pK_a$ for $\mathbf{3}_{ox}$ (Scheme II, reaction b) has been assumed to apply to the formation of 4a-**3**-OOH and the $pK_a$ of the hydroperoxide function of 4a-**3**-OOH is ~9.2.[32] In accord with the cartoon of Figure 8, $\mathbf{3}_{ox}$ is known to react with $H_2O_2$ to yield 4a-**3**-OOH. This is the basis of a preparative procedure for 4a-**3**-OOH.[4] In addition, $O_2^{-}\cdot$ has previously been shown to react with $\mathbf{3}_{rad}$ to yield 4a-**3**-$OO^-$.[9] That the rate-controlling step in the overall $O_2$ oxidation of $\mathbf{3}_{red}$ is the one-electron transfer that

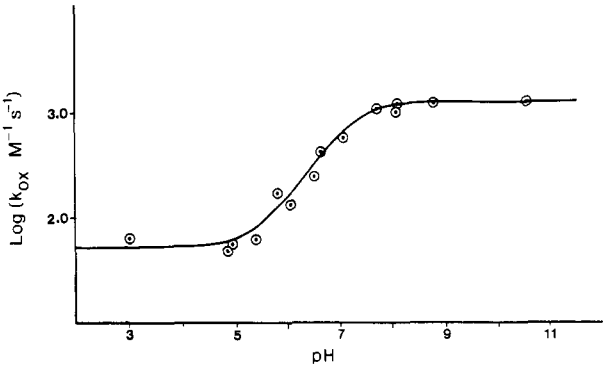


**Figure 10.** Plot of the pH dependence of the log of the second-order rate constants for reaction of $\mathbf{3}_{red}$ with $O_2$. The points are experimental and the line represents the best fit of eq 28c.

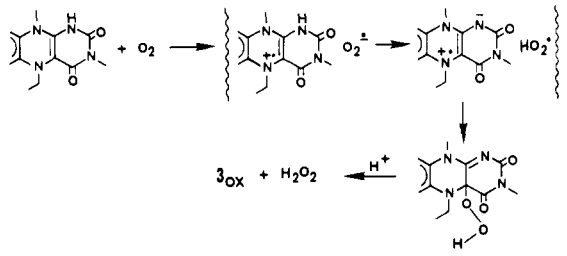


(27)

yields $\{\mathbf{3}_{red}\ O_2^{-}\cdot\}$ is shown by the contents of Figure 9. In Figure 9 there is plotted the pH dependence of $\Delta G°$ for the formation of $\mathbf{3}_{rad}$ and superoxide from $\mathbf{3}_{red} + O_2$ and the pH dependence of $\Delta G^{\ddagger}$ for the reaction of $\mathbf{3}_{red}$ with $O_2$. Inspection of Figure 9 shows that the pH dependences of $\Delta G°$ and $\Delta G^{\ddagger}$ are parallel between pH 3 and pH 10.2 with $\Delta G^{\ddagger} - \Delta G° = 15$ kJ $M^{-1}$. The value of 15 kJ $M^{-1}$ provides a rate constant for $10^{10}$ $s^{-1}$ for the back-reaction of superoxide with flavin radical. The shape of the $\Delta G°$ profile is determined by the pH dependence of the half-cell reactions of eq 16a and 26b. Thus, the calculated values of $\Delta G°$ reflects the protonic equilibria of the acid/base pairs $O_2^{-}\cdot/HO_2\cdot$ ($pK_a = 4.6$), $\mathbf{3}_{rad}\cdot/\mathbf{3}_{rad}^{+}\cdot$ ($pK_a \sim 2$, Scheme II, reaction a), and $\mathbf{3}_{red}/\mathbf{3}_{red}^{-}$ ($pK_a = 6.2$, Scheme II, reaction d). The values of $\Delta G°$ should have little meaning in the construction of a reaction coordinate unless the reactant (dihydroflavin) and product (the intermediates superoxide and flavin radical) are in acid/base equilibria or the rate constants for the reaction of dihydroflavin and dihydroflavin anion are of such values that the superoxide species ($O_2^{-}\cdot$ and $HOO\cdot$) and flavin radical species ($\mathbf{3}_{rad}\cdot$ and $\mathbf{3}_{rad}^{+}\cdot$) are formed in the mole fractions at a given pH that would be present if these species were in acid/base equilibria. The back-rate of $10^{10}$ $s^{-1}$ for conversion of intermediate flavin radical and superoxide to dihydroflavin and $O_2$ precludes the intermediates from being in acid/base equilibria with the buffered solution. The correct explanation is found in the balance of the second-order rate constants of eq 28. In Figure

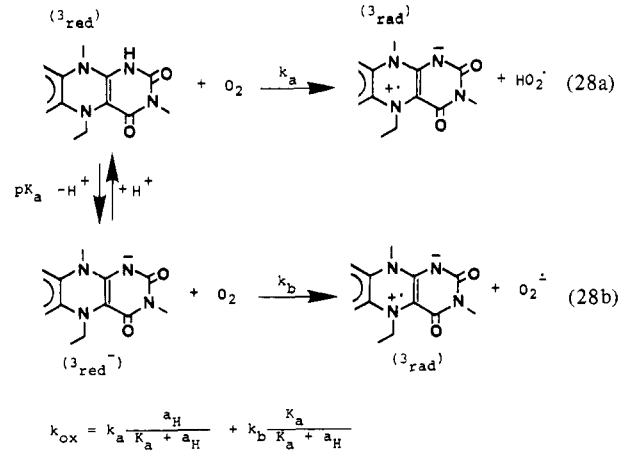


(28a)

(28b)

10 there is plotted log $k_{ox}$ vs. pH. The points are experimental (taken from the paper by Kemal et al.[4] and from his research note book) and the line generated from eq 28c. The value of the determined constants are $k_a = 52$ $M^{-1}$ $s^{-1}$, $k_b = 1.3 \times 10^3$ $M^{-1}$ $s^{-1}$, and $pK_a = 7.04$ (the thermodynamic $pK_a$ has been determined as 6.4[23]). Thus, reactions 28a and 28b have been shown to yield, as short-lived intermediates, $\{\mathbf{3}_{rad}\ HO_2\cdot\}$ and $\{\mathbf{3}_{rad}\ O_2^{-}\cdot\}$ as predicted by the kinetic expression 28c. There can be not doubt about the validity of the one-electron reduction of $O_2$ as the first step in the reaction of dihydroflavin with $O_2$. The sameness in the shape of the pH profile for $\Delta G°$ and $\Delta G^{\ddagger}$ provides strong evidence against a concerted mechanism for 4a-**3**-$OO^{-}$ formation. Most interesting is the observation that the one-electron reduction of $O_2$ by way of the terms $k_a[\mathbf{3}_{red}][O_2]$ and $k_b[\mathbf{3}_{red}^{-}][O_2]$ is such that the ratio of $HO_2\cdot/O_2^{-}\cdot$ produced is predictable from the $pK_a$ of $HO_2\cdot$.

**The reaction of the $N^5$-blocked 1,5-dihydroisoalloxazine $\mathbf{4}_{red}$ and**

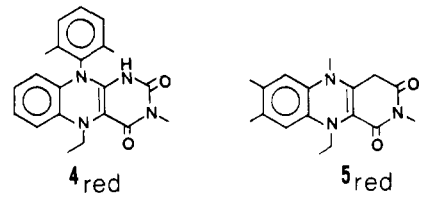


**the 1,5-dihydro-1-carba-1-deazaflavin $\mathbf{5}_{red}$ with $O_2$** can also be discussed in terms of the reaction coordinate cartoon of Figure 8B. The flavin **5** is a 1-carba-1-deaza analogue of **3**.[5c] As in the case of $\mathbf{3}_{red}$, the reaction of $\mathbf{4}_{red}$ and $\mathbf{5}_{red}$ with $O_2$ in polar organic solvents has been shown to yield 4a-**4**-OOH and 4a-**5**-OOH, respectively.[5c,35] The compound $\mathbf{4}_{red}$ is sterically blocked at the 10a-position and has been employed to show that the hydroperoxy moiety of 4a-**4**-OOH does not migrate from the 4a- to the 10a-position.[35,36]

The free energies of activation for reaction of $\mathbf{3}_{red}$, $\mathbf{4}_{red}$, and $\mathbf{5}_{red}$ with $O_2$ are quite similar [$\Delta G^{\ddagger}$ (pH 4.6) 64 kJ $M^{-1}$ for $\mathbf{3}_{red}$, 71 kJ $M^{-1}$ for $\mathbf{4}_{red}$, and 65 kJ $M^{-1}$ for $\mathbf{5}_{red}$]. In separate experiments there were determined, by thin-layer cyclic voltammetry, the two one-electron potentials for reduction of isoalloxazines **4** and **5**. These were found to be clearly separable as shown for **3** in Figure 2B (eq 29 and 30). The free energies of eq 31 and 32 were

| | $E_0$ (pH 4.6) | |
|---|---|---|
| $\mathbf{4}_{ox} + 1e^{-} \rightarrow \mathbf{4}_{rad}$ | 365 mV | (29a) |
| $\mathbf{4}_{rad} + 1e^{-} \rightarrow \mathbf{4}_{red}$ | 230 mV | (29b) |
| | $E_0$ (pH 4.6) | |
| $\mathbf{5}_{ox} + 1e^{-} \rightarrow \mathbf{5}_{rad}$ | 295 mV | (30a) |
| $\mathbf{5}_{rad} + 1e^{-} \rightarrow \mathbf{5}_{red}$ | 135 mV | (30b) |

calculated by using eq 29b, 30b, and 16.

$$\mathbf{4}_{red} + O_2 \rightleftharpoons \mathbf{4}_{rad} + O_2^{-}\cdot \qquad \Delta G° \text{ (pH 4.6)} = 52 \text{ kJ } M^{-1} \quad (31)$$

$$\mathbf{5}_{red} + O_2 \rightleftharpoons \mathbf{5}_{rad} + O_2^{-}\cdot \qquad \Delta G° \text{ (pH 4.6)} = 43 \text{ kJ } M^{-1} \quad (32)$$

These data allow the calculation of the rate constant of eq 33 and 34.

$$\mathbf{4}_{red} + O_2 \underset{1 \times 10^9\ s^{-1}}{\overset{4.2\ M^{-1}\ s^{-1}}{\rightleftharpoons}} \mathbf{4}_{rad}\ O_2^{-}\cdot \quad (33)$$

$$\mathbf{5}_{red} + O_2 \underset{2 \times 10^9\ s^{-1}}{\overset{42\ M^{-1}\ s^{-1}}{\rightleftharpoons}} \mathbf{5}_{rad}\ O_2^{-}\cdot \quad (34)$$

The standard free energies of eq 35 and 36 are also calculable.

$$\mathbf{4}_{red} + O_2 \rightleftharpoons \mathbf{4}_{ox} + H_2O_2 \qquad \Delta G° \text{ (pH 4.6)} = -29 \text{ kJ } M^{-1} \quad (35)$$

$$\mathbf{5}_{red} + O_2 \rightleftharpoons \mathbf{5}_{ox} + H_2O_2 \qquad \Delta G° \text{ (pH 4.6)} = -45 \text{ kJ } M^{-1} \quad (36)$$

From these computations it can be seen that the free energy content of $\mathbf{4}_{rad} + O_2^{-}\cdot$ and $\mathbf{5}_{rad} + O_2^{-}\cdot$ are, as shown previously

(35) Miller, A.; Bruice, T. C. *J. Chem. Soc., Chem. Commun.* **1979**, 896.
(36) Bruice, T. C.; Miller, A. *J. Chem. Soc., Chem. Commun.* **1980**, 693.

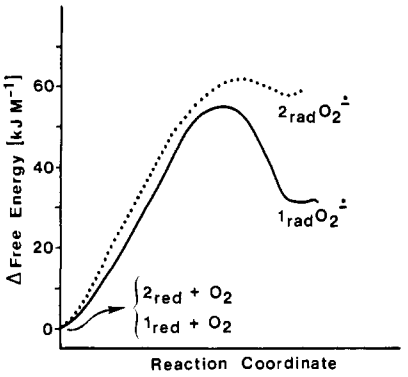


**Figure 11.** Comparison of the reaction coodinants for reduction of $O_2$ to $O_2^{-}\cdot$ by $\mathbf{1}_{red}$ and $\mathbf{2}_{red}$ in water at pH 4.6 (30 °C).

in the oxidation of $\mathbf{2}_{red}$ and $\mathbf{3}_{red}$, somewhat less than the free energies of activation for $O_2$ oxidation of $\mathbf{4}_{red}$ and $\mathbf{5}_{red}$. The transition states for the $O_2$ oxidation of $\mathbf{4}_{red}$ and $\mathbf{5}_{red}$ (71 and 63 kJ $M^{-1}$, respectively) resemble closely the intermediate radical pairs. Differences in the reaction coordinant diagrams for oxygen reacting with $\mathbf{3}_{red}$ vs. those for oxygen reacting with $\mathbf{4}_{red}$ and $\mathbf{5}_{red}$ reside primarily in the greater overall standard free energies for product formation in the latter reactions.

**Equations 37–39 are important in the discussion of the reaction of the $N^1$-blocked 1,5-dihydroflavin $\mathbf{1}_{red}$ with oxygen at pH 4.6 (Scheme III).**

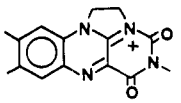


(37)

$$\mathbf{1}_{rad} + 1e^- \rightarrow \mathbf{1}_{red} \qquad E_0 \text{ (pH 4.6)} = 145 \text{ mV} \qquad (38)$$

$$\mathbf{1}_{red} + O_2 \xrightarrow{1.5 \times 10^3\ M^{-1}\ s^{-1}} \mathbf{1}_{ox} + H_2O_2 \qquad \Delta G^{\ddagger} \text{ (pH 4.6)} = 54.9 \text{ kJ } M^{-1} \qquad (39)$$

Combining eq 37 and 38 with eq 16 provides eq 40–42.

$$\mathbf{1}_{red} + O_2 \rightarrow \mathbf{1}_{rad} + O_2^{-}\cdot \qquad \Delta G^{\circ} \text{ (pH 4.6)} = 44 \text{ kJ } M^{-1} \qquad (40)$$

$$\mathbf{1}_{rad} + O_2^{-}\cdot \rightarrow \mathbf{1}_{ox} + H_2O_2 \qquad \Delta G^{\circ} \text{ (pH 4.6)} = -116 \text{ kJ } M^{-1} \qquad (41)$$

$$\mathbf{1}_{red} + O_2 \rightarrow \mathbf{1}_{ox} + H_2O_2 \qquad \Delta G^{\circ} \text{ (pH 4.6)} = -72 \text{ kJ } M^{-1} \qquad (42)$$

Replacement of the $N^5$-ethyl group of $\mathbf{2}_{rad}$ with a proton to provide $\mathbf{1}_{rad}$ is accompanied by a decrease in the one-electron reduction potential by 140 mV (eq 11 vs. eq 38). Thus, $\mathbf{1}_{red}$ is a much better reducing agent than is $\mathbf{2}_{red}$ and the rate of $O_2$ reduction by $\mathbf{1}_{red}$ should exceed the rate of $O_2$ reduction by $\mathbf{2}_{red}$. Likewise, $\mathbf{2}_{rad}$ should be a better oxidant of $O_2^{-}\cdot$ than $\mathbf{1}_{rad}$. These expectations are supported by the experimental data at pH 4.6 as shown in Figure 11. Whereas the rate constant for oxidation of $O_2^{-}\cdot$ by $\mathbf{2}_{rad}$ is calculated to be $\sim 10^{11}$ $M^{-1}$ $s^{-1}$, the rate constant for oxidation of $O_2^{-}\cdot$ by $\mathbf{1}_{rad}$ is $\sim 2 \times 10^8$ $M^{-1}$ $s^{-1}$. In the case of the reduction of $O_2$ by $\mathbf{2}_{red}$ the intermediates $\mathbf{2}_{rad}$ and $O_2^{-}\cdot$ are forced to exist as a transient radical ion pair ($\{\mathbf{2}_{rad}\ O_2^{-}\cdot\}$). If, however, the initially formed $\{\mathbf{1}_{rad}\ O_2^{-}\cdot\}$ species does not collapse by radical coupling at a rate greater than $10^8$ $s^{-1}$, these species may diffuse apart. The standard free energy for formation of $\mathbf{1}_{ox} + H_2O_2$ from $\mathbf{1}_{red} + O_2$ (eq 42) at pH 4.6 is sufficiently negative that the only restriction that can be placed on the timing of proton transfer in the reaction of $\mathbf{1}_{red}$ with $O_2$ is that $O_2^{-}\cdot$ cannot be protonated by lyate species or buffer. A reasonable mechanism is depicted in eq 43. The $pK_a$ for $H^+$ dissociation from the radical is 4.4 (Scheme III, reaction a).

**The reaction of $O_2$ with unblocked 1,5-dihydroisoalloxazines may now be considered.** Below the $pK_a$ of the $N^3$–H position of the isoalloxazine ring system, the pH dependences of the electrochemical potentials of tetraacetylriboflavin, flavin mononucleotide (FMN), 3-(carboxymethyl)lumiflavin, lumiflavin, and

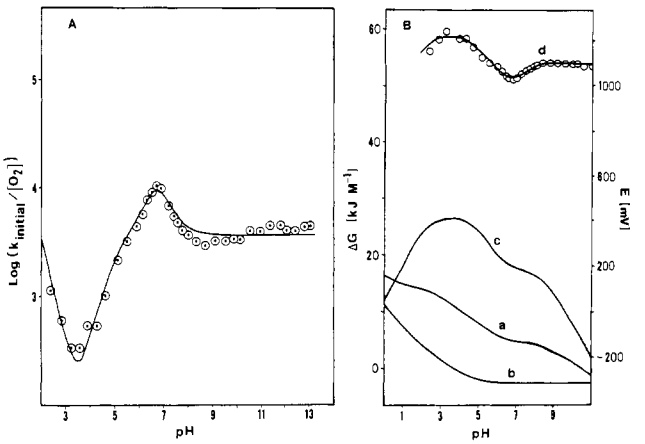


**Figure 12.** (A) The pH profile for the "second-order" rate constants for reaction of $O_2$ with 1,5-dihydroflavin mononucleotide (1,5-$FMNH_2$). The points are experimental and have been taken from ref 2, and the line represents the best fit of eq 49. (B) The points of line d represent values of $\Delta G^{\ddagger}$ calculated from the "second-order" rate constants for reaction of 1,5-$FMNH_2$ with $O_2$. Line c is the pH dependence of $\Delta G$ for the one-electron reduction of $O_2$ by 1,5-$FMNH_2$. The values of $\Delta G$ were calculated from the pH dependencies of the $E_m$ for one-electron reduction of FMN radical (line a) and the one-electron reduction of $O_2$ (line b).

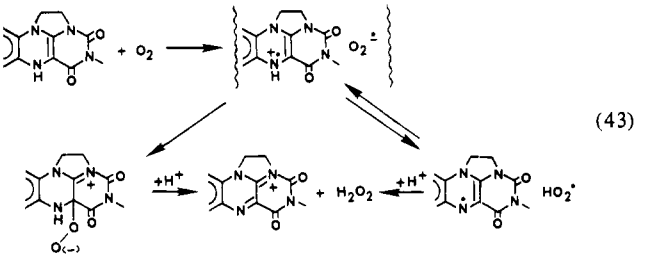


(43)

3-methyllumiflavin are virtually identical (Scheme I; Figure 2A). The abbreviations of eq 1–3 may be employed for these flavins: $FlH_T\cdot = FlH_2^{+}\cdot + FlH\cdot + Fl^{-}\cdot$ and $FlH_T = FlH_2 + FlH^{-}$. The $pK_a$ values associated with the protonic equilibria of oxidized, radical, and 1,5-reduced flavins of this nature are provided in Scheme I. From eq 45 and eq 16a there follows eq 46. The

$$Fl_{ox} + 1e^- \rightarrow Fl_T\cdot \qquad E_0 \text{ (pH 4.6)} = -125 \text{ mV} \qquad (44)$$

$$Fl_T\cdot + 1e^- \rightarrow FlH_T \qquad E_0 \text{ (pH 4.6)} = -45 \text{ mV} \qquad (45)$$

$$FlH_T + O_2 \rightarrow FlH_T\cdot + O_2^{-}\cdot \qquad \Delta G^{\circ} \text{ (pH 4.6)} = 26 \text{ kJ } M^{-1} \qquad (46)$$

second-order rate constant for the reaction of 1,5-dihydro-3-(carboxymethyl)lumiflavin with $O_2$ has been determined to be 417 $M^{-1}$ $s^{-1}$ at pH 4.6. The value of the second-order rate constant for reaction of 1,5-dihydro-FMN with $O_2$ has been reported by Favaudon[2] as $10^3$ $M^{-1}$ $s^{-1}$ at pH 4.6 (initial rates employed in these calculations). The activation energies for these reactions are then 59 and 57 kJ $M^{-1}$, respectively. From these values there follows eq 47 (pH 4.6). The rates for one-electron transfer from $FlH_T\cdot$

$$FlH_T + O_2 \underset{(1-3) \times 10^7\ M^{-1}\ s^{-1}}{\overset{417-10^3\ M^{-1}\ s^{-1}}{\rightleftharpoons}} FlH_T\cdot + O_2^{-}\cdot \qquad (47)$$

to $O_2^{-}\cdot$ are sufficiently small to allow diffusion apart of $FlH_T\cdot$ and $O_2^{-}\cdot$ species. Whether or not this occurs is dependent upon the rate constant for coupling of $FlH_T\cdot$ and $O_2^{-}\cdot$ within the radical pair $\{FlH_T\cdot\ O_2^{-}\cdot\}$. From eq 16, 44, and 45 there is obtained the standard free energy of eq 48. The separation in free energy

$$FlH_T + O_2 \rightarrow Fl_{ox} + H_2O_2 \qquad \Delta G^{\circ} \text{ (pH 4.6)} = -102 \text{ kJ } M^{-1} \qquad (48)$$

content between critical transition state and products is 160 kJ $M^{-1}$. For this reason the only kinetic restriction that can be placed upon proton transfer to an oxygen species in going from $O_2$ to

$H_2O_2$ is that proton transfer may not occur to $\{Fl_T \cdot O_2^- \cdot\}$. The initial radical pair may diffuse apart or collapse to give 4a-hydroperoxyflavin.

Favaudon[2] has provided the pH dependence for the initial rates of reaction of 1,5-dihydro-FMN with $O_2$. These are plotted in the form of log $k_{initial}/O_2$ vs. pH in Figure 12A. In Figure 12B there is plotted, as a function of pH, values of $\Delta G^{\ddagger}$ (from the points of Figure 12A) and $\Delta G°$ for the formation of FMN radical and superoxide. The values of $\Delta G^{\ddagger}$ and $\Delta G^0$ have a constant separation of ~30 kJ $M^{-1}$ between pH 2 and pH 7. In the pH profile of Figure 12A, the line has been generated from eq 44 by employing the rate constants $k_1 = 52\ M^{-1}\ s^{-1}$, $k_2 = 404\ s^{-1}$, and $k_3 = 0.54\ s^{-1}$ (at $[O_2] = 1.5 \times 10^{-3}$ M) and the acid dissociation constants $pK_{a_1} = 9.17$, $pK_{a_2} = 4.34$, and $pK_{a_3} = 4.94$. The values of the kinetically apparent acidity terms $pK_{a_2}$ and $pK_{a_3}$ do not correspond to $pK_a$ values of 1,5-dihydro-FMN, FMN radical, or FMN nor to the (anticipated) $pK_a$ of any intermediate hydroperoxide. The $pK_{a_3}$ value does not approximaae that of $HO_2\cdot$. As recognized by Favaudon, the bimolecular rate constant for the reaction of 1,5-dihydro-FMN with $O_2$ cannot be separated from the ensuing autocatalytic reaction by the use of initial rate constants. It is likely that one or all the acid dissociation constants of eq 49 are

$$\frac{k_{initial}}{[O_2]} = \underbrace{k_1 a_H}_{A} + \underbrace{\frac{k_2 K_{a_1} a_H}{K_{a_1}K_{a_2} + K_{a_1}a_H + a_H^2}}_{B} + \underbrace{\frac{k_3 K_{a_3}}{K_{a_3} + a_H}}_{C} \quad (49)$$

only apparent acid dissociation constants and are composed of kinetic constants related to the autocatalytic reaction.

**Acknowledgment.** This work was supported by grants from the National Science Foundation and from the National Institutes of Health.

**Registry No.** $\mathbf{1}_{red}$, 25431-13-4; $\mathbf{2}_{red}$, 80720-87-2; $\mathbf{3}_{red}$, 50387-36-5; $\mathbf{4}_{red}$, 86969-35-9; $\mathbf{5}_{red}$, 79075-88-0; 3-methyllumiflavin, 18636-32-3; 3-(carboxymethyl)lumiflavin, 20227-26-3; tetraacetylriboflavin, 752-13-6.

# Cross Polarization and Magic Angle Sample Spinning NMR Spectra of Model Organic Compounds. 3. Effect of the $^{13}C$–$^1H$ Dipolar Interaction on Cross Polarization and Carbon–Proton Dephasing

**Lawrence B. Alemany, David M. Grant,* Terry D. Alger, and Ronald J. Pugmire**

*Contribution from the Department of Chemistry, University of Utah, Salt Lake City, Utah 84112.* *Received May 13, 1982*

**Abstract:** Carbon-13 NMR studies involving conventional cross polarization and dipolar dephasing techniques at a variety of contact and delay times, respectively, provide valuable information on the magnitude of $^{13}C$–$^1H$ dipole–dipole interactions. In solids whose spectra have overlapping resonances, such techniques discriminate between protonated and nonprotonated carbons. In dipolar dephased spectra, dipolar and rotational modulation of the resonances can occur for methine and methylene carbons, which are strongly coupled to the directly bonded protons. Methyl carbons exhibit a very wide range of effective dipolar couplings because of rapid methyl rotation that varies depending upon the structural environment. Dipolar modulation in methyl groups is not observed. Carbon atoms in *tert*-butyl methyl groups experience even weaker effective dipolar interactions than other methyl carbon atoms. These motionally decreased dipolar interactions are similar to those experienced by the quaternary aliphatic carbon atom. Steric crowding of a *tert*-butyl group on an aromatic ring causes (on the average) one of its methyl groups to differ in mobility from the other two. A biexponential decay not evident in any of the other functional groups studied results for both the quaternary and methyl carbons in the *tert*-butyl group. Nonprotonated $sp^2$-hybridized carbon atoms also exhibit weak dipolar couplings because of the remoteness of protons. The magnitude of the coupling varies substantially as a result of variations in motional freedom and structure.

## Introduction

Previous work has shown CP/MAS NMR to be very useful for characterizing and quantitatively studying diamagnetic organic solids.[1,2] The relative polarization rates of different types of protonated carbon atoms were shown to be a direct manifestation of the effective magnitude of the $^{13}C$–$^1H$ dipolar interaction. Methyl carbons are especially interesting because they exhibit a wide range of effective dipolar couplings resulting from differing degrees of motional freedom. Conventional cross polarization of a carbon is characterized by the time a carbon nucleus receives polarization from the coupled protons.

Alla and Lippmaa[3] were the first to use dipolar dephasing to distinguish between carbon atoms with different effective dipolar couplings. Since then, the method has been applied to single resonances while producing a spectrum of only minimally attenuated signals for methyl and nonprotonated carbon atoms. In the crystals,[4–6] calcium formate and frozen benzene,[7] simple powdered organic compounds,[8–18] biochemical materials,[9,13,19–23] a clathrate,[24] organometallic complexes,[25,26] polymers,[27–34] and fossil fuel sam-

(1) Part 1: Alemany, L. B.; Grant, D. M.; Pugmire, R. J.; Alger, T. D.; Zilm, K. W. *J. Am. Chem. Soc.* **1983**, *105*, 2133–2141.
(2) Part 2: Alemany, L. B.; Grant, D. M.; Pugmire, R. J.; Alger, T. D.; Zilm, K. W. *J. Am. Chem. Soc.* **1983**, *105*, 2142–2147.
(3) Alla, M.; Lippmaa, E. *Chem. Phys. Lett.* **1976**, *37*, 260–264.
(4) Hester, R. K.; Ackerman, J. L.; Neff, B. L.; Waugh, J. S. *Phys. Rev. Lett.* **1976**, *36*, 1081–1083.
(5) Rybaczewski, E. F.; Neff, B. L.; Waugh, J. S.; Sherfinski, J. S. *J. Chem. Phys.* **1977**, *67*, 1231–1236.
(6) Bodenhausen, G.; Stark, R. E.; Ruben, D. J.; Griffin, R. G. *Chem. Phys. Lett.* **1979**, *67*, 424–427.
(7) Stoll, M. E.; Vega, A. J.; Vaughn, R. W. *J. Chem. Phys.* **1976**, *65*, 4093–4098.
(8) Opella, S. J.; Frey, M. H. *J. Am. Chem. Soc.* **1979**, *101*, 5854–5856.
(9) Opella, S. J.; Frey, M. H.; Cross, T. A. *J. Am. Chem. Soc.* **1979**, *101*, 5856–5857.
(10) Gray, G. A.; Hill, H. D. W. *Ind. Res. Dev.* **1980**, *22* (3), 136–140.
(11) Munowitz, M. G.; Griffin, R. G.; Bodenhausen, G.; Huang, T. H. *J. Am. Chem. Soc.* **1981**, *103*, 2529–2533.

0002-7863/83/1505-6697$01.50/0 